TRIBHUVAN UNIVERSITY
INSTITUTE OF ENGINEERING
PULCHOWK CAMPUS

INVESTIGATION OF EFFECT OF PRINTING PARAMETERS AND REINFORCEMENT ON THE MECHANICAL PROPERTIES OF 3D PRINTED POLYLACTIC ACID (PLA+) COMPOSITES

By:
Kamal Karki (077BAS016)
Krishna Niroula (077BAS017)
Rajeev Kunwar (077BAS031)
Rejin Baral (077BAS033)

A Final Year Project Report
SUBMITTED TO THE DEPARTMENT OF MECHANICAL AND AEROSPACE ENGINEERING IN PARTIAL FULFILLMENT OF THE REQUIREMENT FOR THE DEGREE OF BACHELOR IN AEROSPACE ENGINEERING

DEPARTMENT OF MECHANICAL AND AEROSPACE ENGINEERING
LALITPUR, NEPAL

March 2025

COPYRIGHT

The authors have agreed that the Library, Department of Mechanical and Aerospace Engineering, Institute of Engineering, Pulchowk Campus may make this report freely available for inspection. Moreover, the authors have agreed that permission for extensive copying of this project report for scholarly purpose may be granted by the supervisors who supervised the project work recorded herein or in their absence, by the Head of the Department wherein the project report was done.

It is understood that the recognition will be given to the authors of this project and to the Department of Mechanical and Aerospace Engineering, Pulchowk Campus, Institute of Engineering in any use of the material of this report. Copying or publication or the other use of this report for financial gain without approval of the Department of Mechanical and Aerospace Engineering, Institute of Engineering, Pulchowk Campus and authors' written permission is strictly prohibited. Request for permission to copy or to make any other use of the material in this report in whole or in part should be addressed to:

Head
Department of Mechanical and Aerospace Engineering
Institute of Engineering, Pulchowk Campus
Lalitpur, Nepal

TRIBHUVAN UNIVERSITY
INSTITUTE OF ENGINEERING
PULCHOWK CAMPUS
DEPARTMENT OF MECHANICAL AND AEROSPACE ENGINEERING

The undersigned certify that they have read, and recommended to the Institute of Engineering for acceptance, a project report entitled **"INVESTIGATION OF EFFECT OF PRINTING PARAMETERS AND REINFORCEMENT ON THE MECHANICAL PROPERTIES OF 3D PRINTED POLYLACTIC ACID (PLA+) COMPOSITES"** submitted by **Kamal Karki, Krishna Niroula, Rajeev Kunwar and Rejin Baral** in partial fulfillment of the requirements for the Bachelor's Degree in Aerospace Engineering.

Supervisor: **Dr. Laxman Poudel**, Professor
Department of Mechanical and Aerospace Engineering
Institute of Engineering, Pulchowk Campus

Supervisor: **Rajesh Kaji Kayastha**, Associate Professor
Department of Mechanical and Aerospace Engineering
Institute of Engineering, Pulchowk Campus

External Examiner: **Ashish Manandhar**, MPC Engineer
Himalayan Airline Pvt. Ltd.

Head of Department : **Dr. Sudip Bhattrai**, Assistant Professor
Department of Mechanical and Aerospace Engineering
Institute of Engineering, Pulchowk Campus

DATE OF APPROVAL: 20 April, 2025

Scanned with CamScanner

TABLE OF CONTENTS

LIST OF TABLES

LIST OF FIGURES

LIST OF ABBREVIATIONS

ABS Acrylonitrile Butadiene Styrene

ASTM American Society for Testing Material

CWPC Continuous wire Polymer Composites

FEA Finite Element Analysis

FDM Fused Deposition Modeling

FFF Fused Filament Fabrication

PLA Poly Lactide

PLA-CF Carbon Fiber reinforced Poly Lactide

UTM Universal Testing Machine

Abstract

The use of 3D printing technology in manufacturing has led to groundbreaking advancements in material design, particularly in enhancing the mechanical properties of polymer-based materials. This study focuses on improving the mechanical strength of PLA+ by reinforcing it with multiple steel wires and investigating their effects on tensile, compressive, and impact strength. Specimens were fabricated in compliance with ASTM D638, D695, and impact test BS-2782 part III standards, while Bambu lab Studio slicing software and ANSYS simulations were utilized to predict mechanical behavior and optimize infill density. The results demonstrate that the combination of steel wire reinforcement and optimized infill density significantly enhances the tensile and compressive strength of PLA+ compared to standard 3D-printed specimens.The impact test results further revealed that different infill patterns influenced impact resistance, with the honeycomb pattern exhibiting the highest energy absorption capacity, followed by gyroid and rectilinear patterns. These findings underscore the potential of reinforced 3D-printed materials for applications where strength and durability are critical, paving the way for innovative material solutions in industries such as aerospace, automotive, and construction.

Keywords: 3D Printing, PLA+, Reinforcement, Tensile Strength, Compressive Strength, Impact Strength, Steel Wire, ASTM Standards, ANSYS Simulation, Infill Density

Acknowledgement

This project is prepared in partial fulfillment of the requirements for the bachelor's degree in Mechanical and Aerospace Engineering.

First and foremost, we express our sincere gratitude towards Prof.Dr.Laxman Poudel, Associate Professor Rajesh Kaji Kayastha, and Assistant Professor Ashish Karki for their tremendous support, invaluable insights, and guidance throughout the completion of this project. Their expertise and encouragement were instrumental in shaping the direction of our research and ensuring its successful completion.

We extend our sincere appreciation to the Department of Mechanical and Aerospace Engineering, Pulchowk Campus, for providing the necessary resources, infrastructure, and opportunities to conduct this research. Special thanks to Assistant Professor Biman Rimal for his support and to Chedi Narayan Sir, our lab assistant, for his coordination and assistance in laboratory equipment operations and test conduction.

This work has greatly benefited from the support of our teachers, seniors, and friends, whose continuous encouragement and assistance have been invaluable during various phases of this project. Their motivation played a crucial role in overcoming challenges and achieving milestones.

A special acknowledgment goes to our families, whose unwavering support and inspiration have been a constant source of strength throughout this journey.

Lastly, we welcome and value any feedback, suggestions, or constructive criticism, as they will help us grow and improve.

This project has been a collaborative and enriching experience, and we are thankful to everyone who contributed directly or indirectly to its success.

CHAPTER 1:
INTRODUCTION

1.1 Background

Additive manufacturing, advancing digital manufacturing, technology advancement has different advantage over conventional manufacturing technique able to produce complex geometries without any tooling, integrated functional parts, lattice structures and multi-material components.

Additive manufacturing has transformed the manufacturing landscape by allowing the creation of complex 3D structures with high precision and minimal material waste. Among the various additive manufacturing techniques, Fused Filament Fabrication (FFF) is widely used due to its accessibility, low cost, and versatility in working with thermoplastic materials. PLA (Polylactic Acid) is one of the most commonly used filaments in FFF, known for its ease of use, biodegradability, and low printing temperature. However, standard PLA exhibits limitations in mechanical properties such as tensile strength and impact resistance, restricting its use in demanding applications.

To overcome these limitations, PLA+ was developed as an enhanced version of PLA, offering improved mechanical performance, including higher tensile strength, toughness, and reduced brittleness. Despite these improvements, the mechanical characteristics of 3D printed parts made from PLA+ are still influenced by various process parameters in the FDM process, such as nozzle temperature, bed temperature, printing speed, infill density, and layer height. A deeper understanding of these parameters is crucial for optimizing the mechanical properties of the printed parts.

1.1.1 Nozzle Temperature

Nozzle temperature is a critical parameter that directly affects the quality, strength, and appearance of the printed object. The nozzle temperature needs to be carefully adjusted based on the type of filament material being used. Different brands might have slight variations in their recommended temperature ranges even for the same material type. Higher print speeds may require a higher nozzle temperature to ensure the filament melts and flows properly. Thicker layers may need a slightly higher temperature to

ensure proper adhesion between layers.

1.1.2 Printing Speed

Printing speed refers to the rate at which the print head moves along the X-axis and Y-axis depositing material to create an object. This is a crucial factor because it impacts how quickly a 3D printer can complete a build. Increasing speed without considering other parameter could lead to material defects, poor adhesion or decreased surface quality. Too slow speed could result in time consumption, particularly reduces productivity.

1.1.3 Layer Thickness

Layer thickness, also known as layer height, is a critical parameter in 3D printing that influences the quality, strength, and print time of the final object. It refers to the height of each individual layer of material that is deposited during the printing process. It is typically measured in millimeters (mm) or microns (µm), with common values ranging from 0.1 mm (100 microns) to 0.3 mm (300 microns) for most consumer-grade 3D printers. Finer Layers (Lower Layer Height): can produces smoother surfaces and finer details. Ideal for objects with intricate details or where surface finish is critical. Thicker Layers (Higher Layer Height) can results in a more noticeable ”stair-stepping” effect on the surface. Suitable for less detailed or functional parts where surface quality is not as important. Finer Layers can produce stronger parts because they allow for better bonding between layers. Thicker Layers may result in weaker layer adhesion, potentially reducing the part’s overall strength.

1.1.4 Infill density

Infill density in 3D printing refers to the internal structure of a printed object, which is essentially a lattice or pattern that fills the hollow space inside the outer shell. It’s a critical parameter because it directly impacts the strength, weight, material usage, and print time of the object. The pattern of the infill can also affect the strength and print time. Common patterns include:

1. Grid: A simple criss-cross pattern that is easy to print and provides decent strength.

2. Honeycomb: A hexagonal pattern that offers a good balance between strength and material usage.
3. Gyroid: A complex pattern that provides excellent strength and material efficiency.
4. Triangles: Strong pattern, good for mechanical parts.
5. Cubic: Provides isotropic strength properties, meaning it is strong in all directions.

1.1.5 Impact Loading

During impact, structures are subjected to high strains over a short period, leading to the conversion of kinetic energy into internal energy. The rate at which the structure returns to its equilibrium state, and how much energy is dissipated, depends on the damping characteristics of the material and structure. Materials with higher damping are more effective at reducing vibrations and can better withstand repeated impacts.

1.1.6 Reinforced Metallic wire properties

The 1.2 mm mild steel wire used for reinforcement significantly enhances the mechanical properties of the 3D-printed parts. With a tensile strength ranging from 400 MPa to 1200 MPa, it provides excellent load-bearing capacity, making the structure more resistant to failure under tension. Additionally, its elastic modulus of approximately 200 GPa ensures high stiffness, reducing deformation under applied loads. The wire's density of 7.85 g/cm³ adds some weight to the printed part, but this trade-off is often justified by the substantial increase in strength. The effectiveness of bonding between the steel wire and the polymer primarily depends on mechanical interlocking, although surface treatments can further enhance adhesion. Overall, the incorporation of carbon steel wire improves the structural integrity and mechanical performance of 3D-printed components, making them more suitable for load-bearing applications.

1.1.7 Finite Element Analysis

Finite Element Analysis(FEA), a numerical method to solve engineering problem, is a versatile and comprehensive numerical technique that provides reliable engineering

solutions. The finite element method is a mathematical procedure based on solving differential equations as best as possible. From an engineering perspective, differential equations are important because they represent the language in which physical laws are expressed. The aim of FEA is to transform the differential equations of the system into a set of linear equations, which can then be solved by computer software.

1.1.8 Regression Analysis

Regression analysis is a statistical method used to model and analyze relationships between dependent and independent variables. It helps in predicting outcomes, understanding relationships, and making data-driven decisions.

1.1.9 Random Forest

Random Forest is a supervised learning algorithm that builds multiple decision trees and combines their outputs to make a final prediction. It reduces overfitting and improves generalization compared to a single decision tree. For classification, it selects the class with the majority votes from all trees. For regression, it averages the outputs of multiple trees.

1.1.10 Polynomial Regression

Polynomial Regression is a type of regression analysis used when the relationship between the independent variable (X) and the dependent variable (Y) is non-linear. Instead of fitting a straight line (as in linear regression), it fits a polynomial curve to capture the underlying trends in the data. A polynomial regression model extends linear regression by adding higher-degree terms of X :

$$Y = \beta_0 + \beta_1 X + \beta_2 X^2 + \beta_3 X^3 + \cdots + \beta_n X^n + \varepsilon$$

Where:

- Y = Dependent variable (response variable).
- X = Independent variable (predictor).
- $\beta_0, \beta_1, \ldots, \beta_n$ = Regression coefficients.

- n = Degree of the polynomial.
- ε = Error term.

1.1.11 Gradient Boosting Regression

Gradient Boosting Regression (GBR) is a powerful machine learning algorithm used for regression tasks. It builds an ensemble of weak learners (decision trees) in a sequential manner, improving performance at each step by minimizing errors. Gradient Boosting minimizes a loss function L by updating predictions iteratively:

$$F_m(X) = F_{m-1}(X) + \gamma h_m(X)$$

Where:

- $F_m(X)$ = Model at iteration m.
- $F_{m-1}(X)$ = Previous model.
- $h_m(X)$ = New weak learner (decision tree) trained to correct residuals.
- γ = Learning rate (controls step size).

The algorithm uses gradient descent to minimize the loss function.

1.2 Problem Statement

Previous studies have investigated the effect of printing parameters such as infill density, print speed, and infill pattern on PLA+ strength. However, there is limited research on other printing parameters and about the effect of reinforcement on the PLA+ specimen. Additionally, while the compressive and impact performance of PLA+ is crucial for structural applications, there is a lack of comprehensive study on how the printing parameters effect the strength. By conducting tensile, compression and impact tests, this research will provide a holistic understanding of the effect of geometric parameter in mechanical performance of 3D-printed PLA+ components. The findings will contribute in enhancing the structural integrity of 3D-printed parts while reducing the cost

as well as predicting the required strength using the minimal amount of filaments making them more suitable for engineering applications that require improved strength and durability at lower cost.

1.3 Objective

1.3.1 Main Objective

The main objective of the project is to study the mechanical performance and structural integrity of 3D-printed PLA+ composites under different conditions.

1.3.2 Specific objective

- To evaluate the influence of printing parameters, including temperature, infill density, and infill pattern on the tensile strength and young's modulus of the printed material.
- To evaluate the different regression analysis and compare it to predict the required strength of the specimen.
- To investigate the effect of metallic wire reinforcement on the mechanical properties of PLA+ composites, including Ultimate tensile strength, and Young's modulus.
- To evaluate the compressive behaviour of 3D-Printed PLA+ at different infill density.
- To analyze the damping characteristics of various structural patterns under impact loading.

1.4 Feasibility Analysis

The project is highly feasible from technical, economic, operational, legal, and environmental perspectives. It also offers significant academic and industrial value in understanding how additive manufacturing parameters and reinforcements affect the mechanical behavior of PLA+ composites.

1.4.1 Technical Feasibility

The design of the specimen is carried out in the CAD software CATIA and Solidworks. PLA+ is a widely available material used in 3D printing, and metallic reinforcements (Mild Steel is used in our project) is also readily accessible. The combination of these materials is technically feasible. Fused Deposition Modeling (FDM) or similar 3D printing techniques can be used to fabricate PLA+ specimens with embedded metallic reinforcements which is fairly feasible. For testing, UTM and other experimental setup can be used. Simulation study of mechanical property of PLA+ and metal reinforced is feasible by using FEM analysis software (ANSYS).

1.4.2 Economic Feasibility

PLA+ is a cost effective material and Mild Steel wire are also easily manageable for our research. For printing of PLA+ specimen and with reinforced metal, printer provided by the department reduced our overall cost. For testing of specimen, the Universal Testing Machine(UTM) and operator is facilitated by the Department of Mechanical and Aerospace Engineering.

1.4.3 Operational Feasibility

Using metallic wire-reinforced PLA+ for 3D printing can boost strength and durability, but it's not as simple as it sounds. PLA+ is easy to print and eco-friendly, but adding metal wires requires careful planning. The wires need to bond well with the plastic during printing, which might mean tweaking printer settings or even upgrading to specialized equipment. Standard 3D printers might not cut it for this kind of project. There is need of a printer that can handle dual materials or one with a modified nozzle to lay down both composites and metal wires. This approach isn't cheap. Upgrading or buying new equipment can be a big investment. This will need training to handle the new equipment properly. Safety is another concern handling metal wires and working with modified printers can pose risks if proper precautions aren't taken. It's not impossible, but it requires careful planning and attention to detail to make it work smoothly.

1.5 System requirement

Different hardware and software were used to make our project run successfully. Below is the list provided:

1.5.1 Hardware requirement

Universal Testing Machine

A Universal testing machine (UTM) is used to test the mechanical properties (tension, compression etc.) of a given test specimen by exerting tensile, compressive or transverse stresses. The machine has been named so because of the wide range of tests it can perform over different kind of materials. Different tests like peel test, flexural test, tension test, bend test, friction test, spring test etc. can be performed with the help of UTM.

Figure 1.1: Universal testing Machine

Bambulab A1 mini 3D-Printer

The Bambu Lab A1 Mini is an entry-level 3D printer designed to make 3D printing accessible and user-friendly. It features a compact design with a build volume of 180 x 180 x 180 mm, making it suitable for various projects.

Figure 1.2: Bambulab A1 Mini

Arduino and MPU6050 Accelerometers Sensor

The Arduino Uno is a widely used microcontroller board based on the ATmega328P, featuring 14 digital I/O pins, 6 analog inputs, and support for UART, SPI, and I²C communication. It operates at 5V with a 16 MHz clock speed and is commonly used for robotics, automation, and IoT projects. The MPU6050 is a 6-axis IMU (Inertial Measurement Unit) that combines a 3-axis accelerometer for measuring linear acceleration and a 3-axis gyroscope for angular velocity. It communicates with the Arduino using the I²C protocol, with the SCL and SDA lines connected to A5 and A4, respectively.

Figure 1.3: Arduino and MPU6050 Schematic

1.5.2 Software requirements

Bambulab Slicing Software

Bambu Lab's slicing software, Bambu Studio, is a powerful and feature-rich slicer based on PrusaSlicer, optimized for Bambu Lab 3D printers. It offers advanced capabilities such as multi-color and multi-material printing, particularly when used with the Automatic Material System (AMS). The software includes adaptive layer height adjustments, custom and tree supports, and fine-tuned settings for high-speed printing.

Arduino IDE

The Arduino Integrated Development Environment (IDE) is an open-source software platform used for writing, compiling, and uploading code to Arduino boards. It provides a simple and user-friendly interface, making it accessible to both beginners and advanced users. The IDE supports a wide range of programming languages, primarily C and C++, and offers a variety of built-in libraries to facilitate hardware interfacing.

Users can write their programs, called sketches, which are then compiled into machine code and uploaded directly to the Arduino board via USB.

Ansys Software

Ansys, like many other FEA programs is also divided into three main parts namely the processors which are called pre-processor, solution processor and post processor. The ansys pre-processor allows user to build geometry, define element and generate element mesh. The ansys processor allows users to solve problem by applying loads and obtaining solution. The ansys post-processors allows visualization and listing of results in tabular form or as printout. Ansys offers a comprehensive software suite that spans the entire range of physics, providing access to virtually any field of engineering simulation that a design process requires.

Python

Python is a versatile programming language widely used for data processing due to its rich ecosystem of libraries and tools. Software like Pandas provides powerful data manipulation capabilities with DataFrames, enabling efficient handling of structured data, while NumPy supports fast numerical computations on arrays and matrices. For larger datasets, tools like Dask or PySpark allow scalable processing across multiple cores or clusters. Libraries such as SciPy and Scikit-learn enhance Python's utility for scientific computing and machine learning tasks, respectively, while Matplotlib and Seaborn offer robust visualization options. Together, these tools make Python an ideal choice for tasks ranging from data cleaning and transformation to advanced analytics and reporting.

CHAPTER 2:
LITERATURE REVIEW

Additive manufacturing, also known as 3D printing, is revolutionizing the manufacturing and prototyping sectors by offering a more straightforward and cost-effective process for product development compared to traditional production methods. Among the various techniques, material extrusion, commonly referred to as fused filament fabrication (FFF), is the most widely adopted and rapidly growing 3D printing technology [1,2]. Stratasys co-founder Scott Crump invented material extrusion in 1989 and patented it.[2] This innovation brought fused deposition modeling (FDM) to the market, initially referred to as FFF. The technology gained widespread recognition following the expi- ration of the Stratasys FDM patent.[3] Despite its advantages, studies indicate that components manufactured using conventional methods exhibit superior mechanical properties compared to those produced through material extrusion. This disparity arises from the layer-by-layer printing pro- cess, which introduces internal gaps and residual stresses during mechanical testing.

Researchers worldwide are addressing this challenge by optimizing process parameters to enhance the mechanical properties of 3D-printed components.[4,5,6] Numerous studies have explored methodologies to improve the process-structure attributes of 3D-printed polymers. Gebisa et al.[4] employed a full factorial design experiment to examine the impact of FFF process parameters on the tensile properties of ULTEM 9085. Their analysis focused on air gap, raster width, raster angle, contour count, and raster width, identifying raster angle as the most significant factor influencing mechanical properties.

Claver et al.[5] investigated the tensile strength of polylac- tic acid (PLA) and acrylonitrile butadiene styrene (ABS) concerning layer height, infill density, and layer orientation. Their findings revealed that while layer height had min- imal impact, infill density significantly influenced tensile strength. Chokshi et al.[6] further examined the effects of layer thickness, infill pattern, and contour number using PLA, highlighting the dominant roles of contour number and layer thickness in deter- mining flexural strength. Similarly, Othman et al.[8] demonstrated that layer thickness, infill pattern,

and contour number collectively contributed to mechanical properties, with infill density being a critical factor. Studies have consistently reported that infill density is a critical parameter affecting mechanical performance. The study conducted by Yılan et al. [9] investigates the influence of these parameters on the tensile strength and production time of PLA+ specimens. The authors highlight that the tensile strength of FDM-printed parts is primarily affected by infill density, which contributes approximately 90.7% to the mechanical performance. Higher infill density results in stronger parts, while lower densities compromise strength. The study also finds that infill patterns influence the homogeneity of internal structures, affecting stress distribution. The triangular infill pattern demonstrated the highest tensile strength at 100% infill density and 40 mm/s print speed, while the gyroid infill pattern resulted in the lowest production time.

Print speed also plays a role in production efficiency. The analysis shows that print speed affects production time by 46.4%, followed by infill density at 28.4%. However, its impact on tensile strength is minimal. The study utilized ANOVA and signal-to-noise ratio analysis to optimize process parameters, confirming that infill density is the most significant factor influencing mechanical performance. The research contributes to the understanding of how FDM process parameters affect the structural integrity of printed parts. The findings reinforce the importance of selecting appropriate infill densities and patterns to achieve optimal mechanical properties in PLA+ components.

To address the limitations of pure polymers, researchers have developed composites by incorporating reinforcing materials such as fibers, particles, or fillers into polymers. These composites exhibit enhanced properties, including greater strength, stiffness, toughness, and wear resistance. Ning et al.[6] evaluated the effects of carbon fibers on the mechanical properties of ABS parts produced via FFF, noting increased tensile strength and Young's modulus but reduced toughness, yield strength, and ductility. Love et al.[7] found that combining carbon fibers and polymers in FFF fabrication improved strength, stiffness, thermal conductivity, and reduced distortion. Similarly, Perez et al.[8] analyzed the reinforcement of ABS with TiO2 at a 5 percent weight ratio, achieving superior ultimate tensile strength. Reinforcement techniques such as fiber embedding, polymer matrix composites, and metal wire integration have been explored to enhance mechanical properties.

Carbon fiber and glass reinforcement have been extensively studied, with results showing significant strength improvements [10][11]. However, these reinforcements require specialized processing conditions, in- creasing manufacturing complexity and costs [12]. Studies on metal wire reinforcement are limited, particularly in the context of cost-effective alternatives like construction- grade coil wire [13][14]. Advanced materials and novel reinforcement techniques have further expanded the potential of additive manufacturing. Aissa et al.[9] investigated reinforced polyamide (RPA) using FFF process parameters such as printing speed, extrusion temperature, and layer thickness. Wu et al.[15] highlighted reinforcement strategies for 3D-printed concrete, demonstrating that vertical steel wire meshing and prefabricated steel significantly enhance flexural strength, ductility, and structural stability. Sanei and Popescu's systematic review[16] emphasized the role of concentric fiber rings and longitudinal fiber alignment in improving fatigue resistance and load-carrying capacity. Additionally, Hematibahar et al.[17] examined the influence of 3D-printed rein- forcement on ultra-high-performance concrete, showing a transition from brittle to duc- tile fracture mechanisms. Maurya et al.[19] demonstrated that incorporating steel cables into 3D-printed samples improved flexural strength by up to 240 percent for certain wire diameters. Jahangir et al.[18] reported that reinforcing polycarbonate (PC) with continuous carbon fiber increased tensile yield strength by 77 percent and modulus of elasticity by 85 percent. Boztoprak et al.[20] found that reinforcing PLA with carbon fiber composites enhanced hardness, tensile strength, bending, impact resistance, and wear properties.

Limited research has been conducted on reinforcing PLA+ with mild steel (MS) wire and analyzing its impact on tensile strength. While PLA is widely studied for its mechanical properties and potential reinforcements, most studies focus on fiber reinforcements such as carbon fiber, glass fiber, or metal powders. However, the direct incorporation of MS wire as a reinforcement material remains relatively unexplored. Investigating its effects could provide valuable insights into how metallic reinforcements influence the mechanical behavior of 3D printed PLA+ structures, particularly in terms of strength, ductility, and failure mechanisms. This research could contribute to developing stronger and more durable composite materials for various engineering applications.

Several studies highlight the influence of printing parameters such as layer height,

infill density, printing orientation, and nozzle temperature on the compressive performance of 3D printed materials. Research has shown that higher infill density and optimized layer orientations significantly enhance the compressive strength of printed parts [21]. Additionally, studies indicate that lower layer heights improve part density, reducing internal voids and increasing compressive load-bearing capacity [22]. Polylactic acid (PLA) is one of the most commonly used thermoplastics in 3D printing due to its biodegradability and ease of processing. Studies indicate that PLA exhibits brittle failure under compressive loads, with minimal plastic deformation before fracture. The compressive strength of PLA can vary based on print settings, but it generally falls between 50-80 MPa [23]. Moreover, research shows that higher printing temperatures improve interlayer adhesion, slightly enhancing compressive resistance [24]. Polyethylene terephthalate glycol (PETG) offers a balance between strength and flexibility, making it a suitable alternative to PLA for compression applications. Unlike PLA, PETG demonstrates significant plastic deformation before failure, providing better energy absorption under compressive loads. Studies suggest that PETG's compressive strength is typically lower than PLA but benefits from improved impact resistance and durability [25]. Carbon fiber-reinforced PLA (PLA-CF) has been studied for its superior mechanical properties compared to standard PLA. Due to the high stiffness of carbon fibers, PLA-CF exhibits enhanced compressive modulus and strength. Research indicates that PLA-CF maintains a more stable deformation pattern under compressive stress, reducing premature brittle failure [26]. However, the distribution of carbon fibers within the polymer matrix influences overall performance, necessitating optimized printing conditions.

Studies analyzing failure mechanisms in 3D-printed structures under compression reveal that crack propagation, interlayer adhesion, and internal porosity are key factors influencing material performance [27]. Researchers have utilized scanning electron microscopy (SEM) to study fracture surfaces, showing that weak interlayer bonding contributes to premature failure in certain materials [28]. Strategies such as post-processing techniques, heat treatment, and annealing have been explored to mitigate these issues and enhance compressive performance. Despite extensive research on the mechanical properties of PLA+ in FDM-based 3D printing, there remains a significant gap in the study of its compressive strength. Most studies have focused on parameters like infill

density, print speed, and infill pattern, but their effect on the compressive behavior of PLA+ has not been thoroughly investigated. Understanding the compressive strength of PLA+ is essential for applications where the material is subjected to compressive loads, such as in support structures and cushioning components. Therefore, future research should explore the compressive performance of PLA+ under varying process parameters to provide a more comprehensive understanding of its structural behavior. he mechanical properties of 3D-printed parts are highly dependent on printing parameters such as layer height, infill density, print speed, and build orientation. Research has demonstrated that optimizing these parameters can lead to significant improvements in impact strength. For instance, adjusting the layer height and infill density has been shown to influence the toughness and energy absorption capacity of 3D-printed materials [29].

Variations in print speed and build orientation can result in different impact resistances due to changes in the bonding quality between layers [30]. The choice of material also significantly affects the impact strength of 3D-printed components.

Acrylonitrile Butadiene Styrene (ABS) is widely used for its toughness and impact resistance, making it suitable for functional and load-bearing applications [31]. Polyethylene Terephthalate Glycol (PETG) offers a balance between strength and flexibility,enhancing its ability to withstand impact forces [32]. Nylon's flexibility and high elongation at break contribute to its superior impact resistance compared to other thermoplastics [33]. The impact strength of these materials can further be optimized through fine-tuning of process parameters, including printing temperature, nozzle size, and layer orientation. In addition to impact resistance, understanding the vibration behavior and damping characteristics of 3D-printed materials is essential for applications involving dynamic loading. The damping ratio is a key parameter that measures a material's ability to dissipate vibrational energy, influencing the structural stability and lifespan of the component. The internal architecture of 3D-printed parts, including infill patterns and densities, significantly affects their vibration behavior. The choice of infill pattern influences the stiffness and natural frequency of 3D-printed components, with certain patterns providing better vibrational stability [34]. Higher infill densities generally lead to increased stiffness and higher natural frequencies, but may reduce the damping capacity [35]. The damping properties of 3D-printed components are influ-

enced by both material selection and printing parameters. Flexible materials such as thermoplastic polyurethane (TPU) exhibit higher damping ratios due to their ability to deform under vibrational loads [36]. Adjustments in layer height, print speed, and infill pattern have been shown to affect the damping properties of printed structures [37]. Studies have shown that a higher damping ratio is achievable in 3D-printed materials with higher layer thickness and certain infill patterns such as honeycomb and gyroid. Moreover, the combination of flexible materials with rigid structures in composite printing can enhance both the strength and damping properties of the final part.

Comparing the vibration and damping behavior of 3D-printed materials with conventional materials provides a benchmark for performance evaluation. Metals generally have lower damping ratios compared to polymers, leading to higher vibration amplitudes under dynamic loading [38]. Polymer matrix composites, on the other hand, exhibit higher damping ratios due to their viscoelastic nature. Studies on carbon nanotube-modified epoxy composites have shown improved damping properties, highlighting the potential for 3D-printed polymer-based materials to match the performance of conventional composites [39]. Similarly, sandwich structures with 3D-printed honeycomb cores have demonstrated enhanced damping due to the interaction between the core and face sheets. Research on sandwich beams with magnetorheological elastomer cores under different loading conditions has shown that the interaction between the core material and the face sheets results in increased energy dissipation and reduced vibration amplitudes [40].

CHAPTER 3:
METHODOLOGY AND FLOWCHART

3.1 Methodology Flowchart

The steps and procedure that we followed during the project are provided below:

3.1.1 Tensile test Flowchart

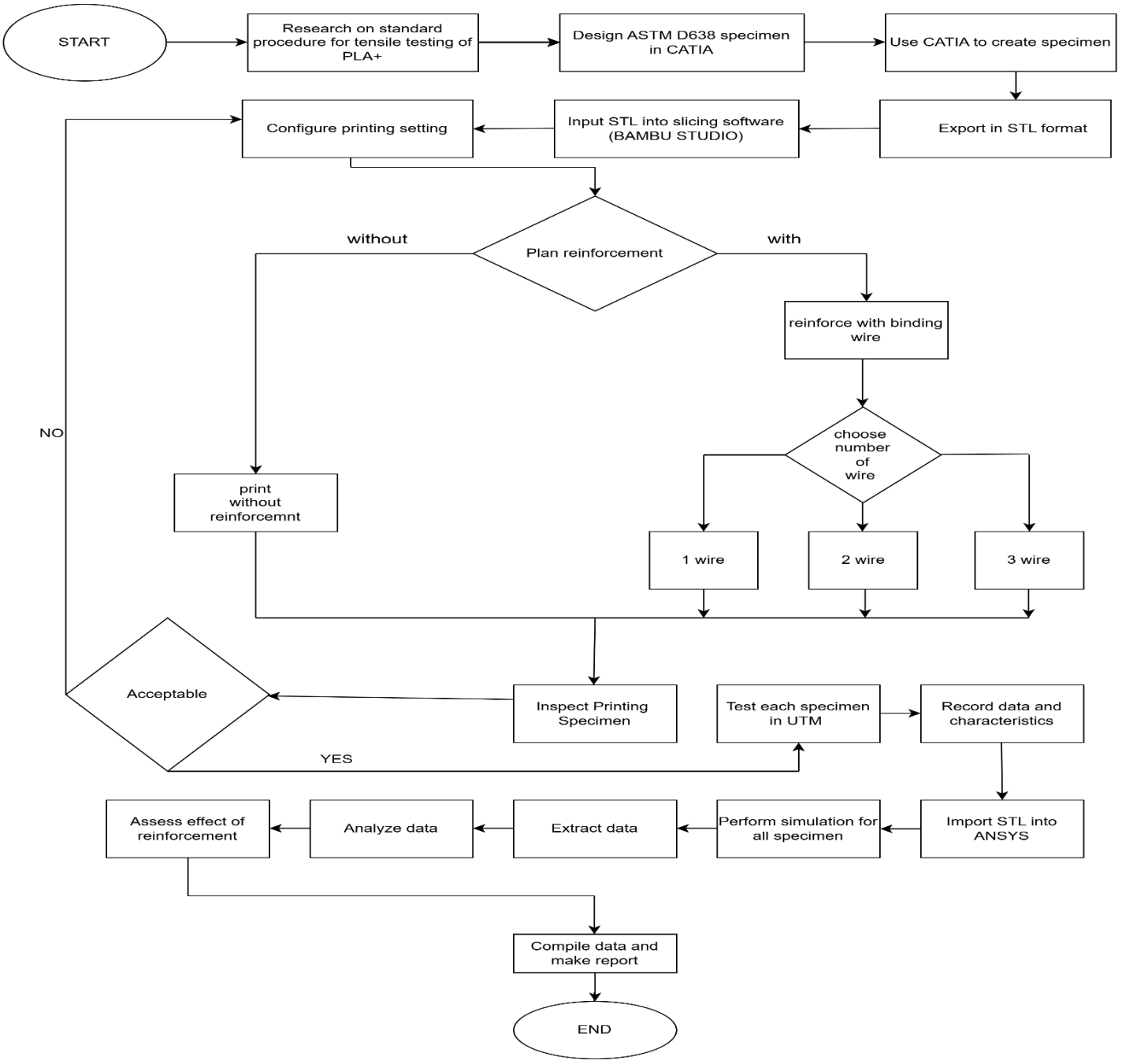

Figure 3.1: Methodology Flowchart

3.1.2 Compression test flowchart

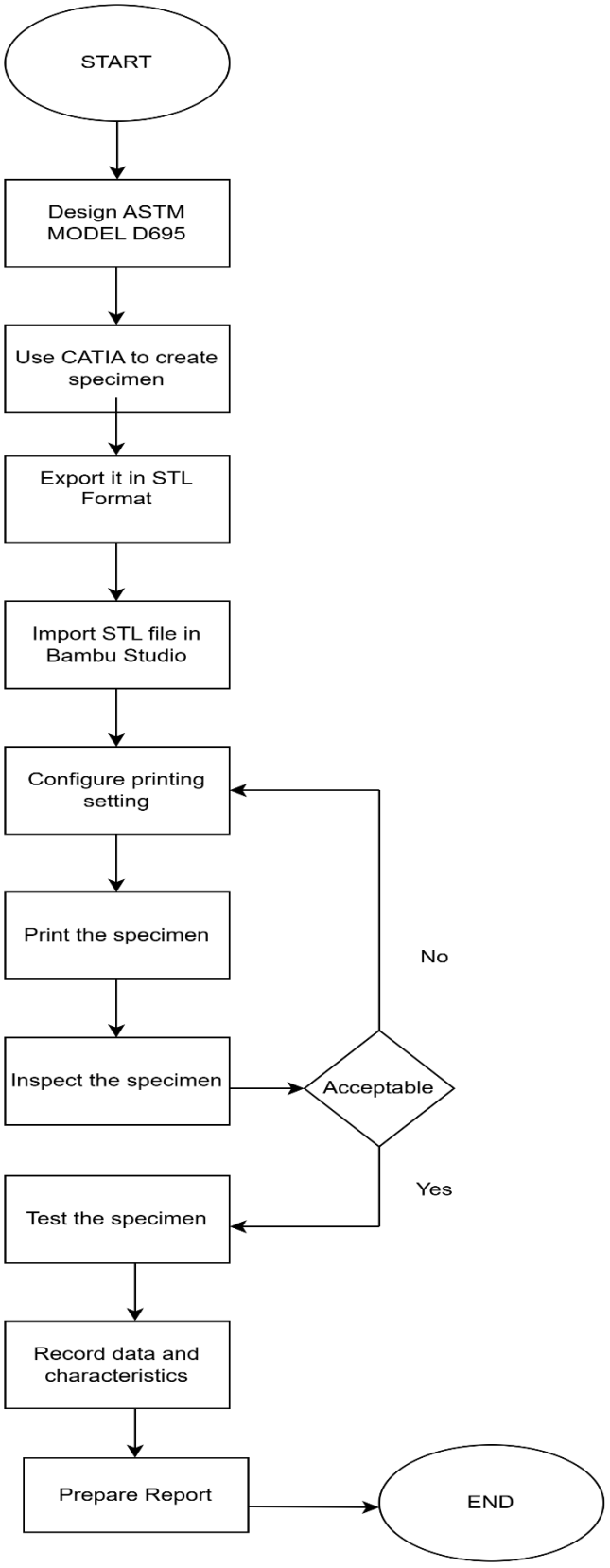

Figure 3.2: Methodology Flowchart

3.1.3 Vibration test flowchart

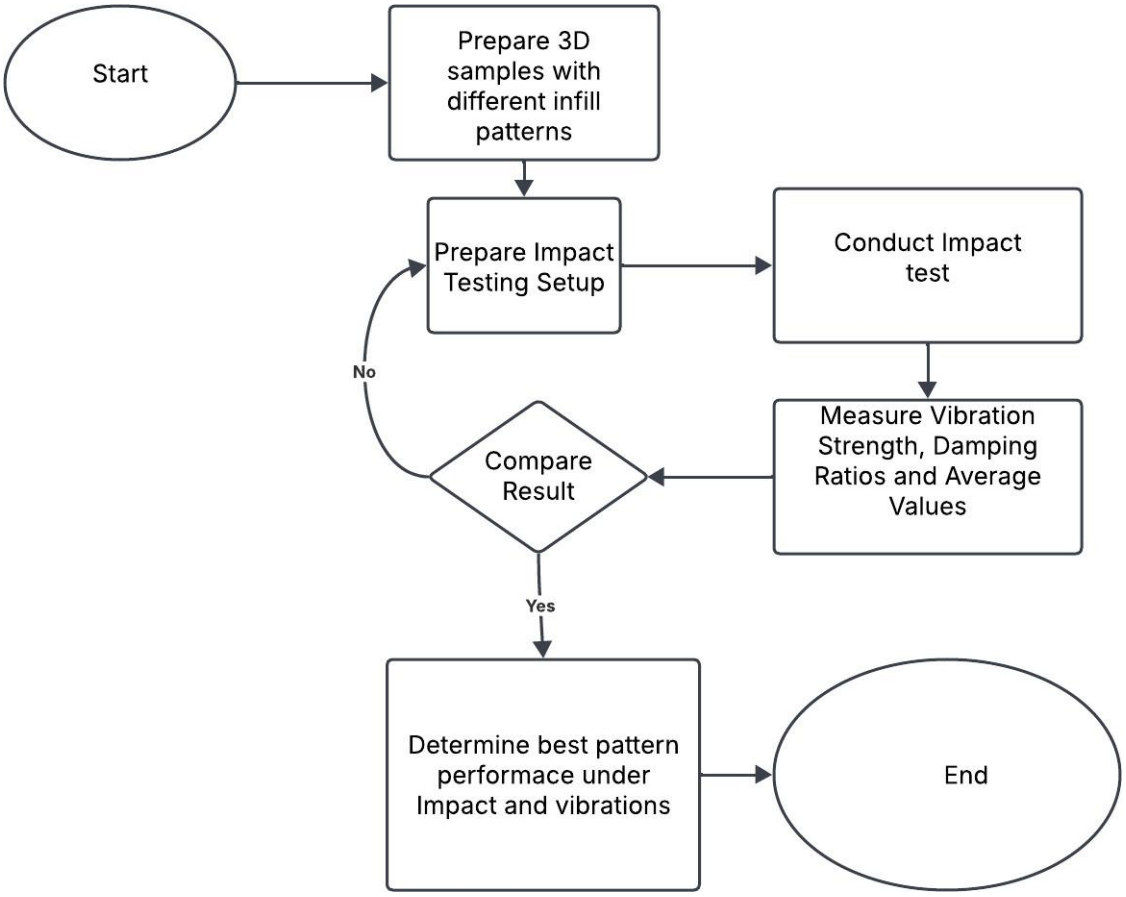

Figure 3.3: Methodology Flowchart

3.2 Developing Computer Aided Design

The CAD model of the specimen is designed in solidworks and saved as STL files. These files then processed using software that generates G-Code for printing the model. The specimens made for tensile test is according to the ASTM D638-14 type I[7] standard method, for compression test is according to the ASTM-D365 standard method and BS 2782 part 3 standard is used to make specimen for testing vibration damping. ASTM D638 method aims to determine the tensile properties of non-reinforced and wire reinforced 3D-printed PLA+ in the form of dog bone structure, tested under specified conditions. Also, ASTM-D365 method aim to determine the compressive strength of non-reinforced 3D-printed PLA+ specimen. The test specimen has an overall length of 165mm and overall width of 19mm, gauge width of 13mm and thickness of 3.6mm.

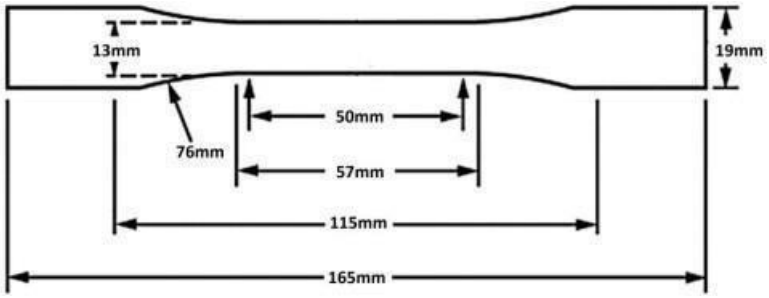

Figure 3.4: Test specimen dimension

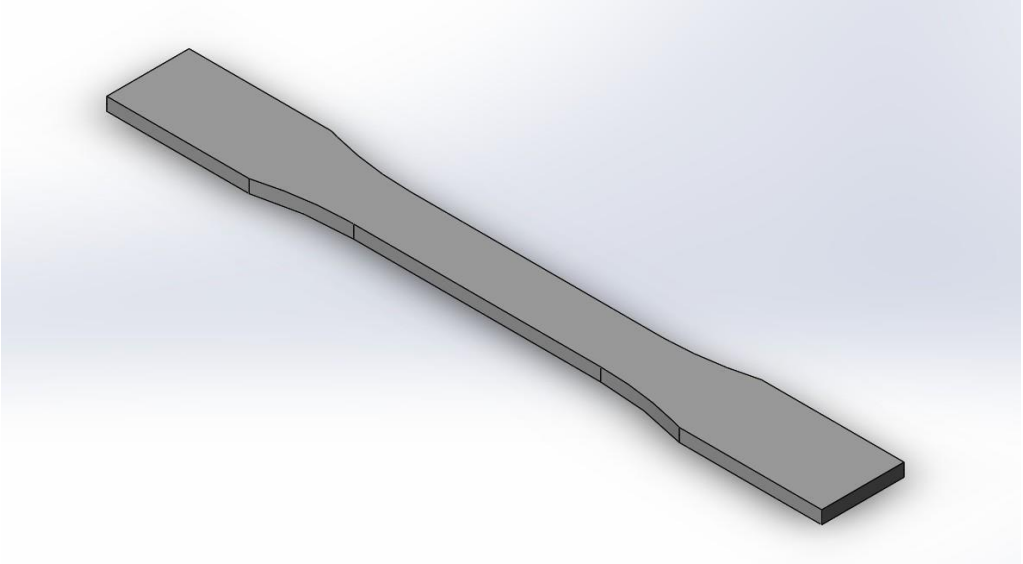

Figure 3.5: CAD model of Specimen

3.3 Choice of Material

PLA+ was selected over standard PLA for this project due to its superior mechanical properties, particularly in terms of tensile strength, impact resistance, and durability. PLA+ typically incorporates additives that enhance its toughness and reduce brittleness, making it more suitable for applications requiring higher structural integrity. Also, less research has been carried out on pla+. Additionally, PLA+ exhibits better layer adhesion in 3D printing, leading to improved overall part strength. Given that the project involves tensile, compressive and tensile testing of ASTM-standard specimens, PLA+ provides a more reliable and consistent material for evaluating mechanical performance, especially when reinforced with additional materials like coil wire and epoxy.

3.4 Slicing of the specimen

Slicing a specimen refers to the process of converting a 3D model into a series of thin, horizontal layers, which can then be printed sequentially by a 3D printer. This process is essential for transforming a digital 3D model into a physical object. The slicer software divides the model into horizontal layers based on the specified layer height. It generates a path for the printer's extruder to follow for each layer, including any infill patterns and supports. The slicing software translates the layer information into G-code, a language that 3D printers understand. G-code contains commands for the printer, including movements, temperature settings, and extrusion rates. Slicing was done on bambu lab software for generating path and G-code for building the material.

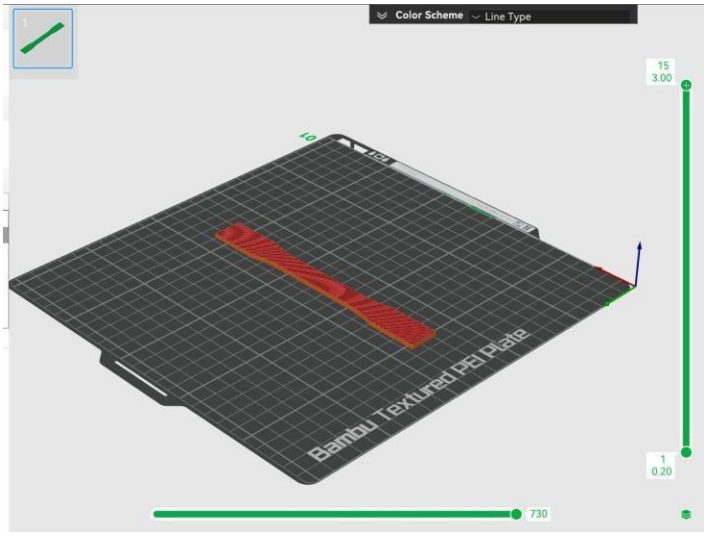

Figure 3.6: Slicing of CAD model

3.5 Design of Experiment

The study consists of majorly influencing parameter such as infill density, Nozzle temperature, layer thickness and printing speed. Inadequate temperature can lead to insufficient adhesion resulting in poor quality of produced material. Large temperature could destroy the structural integrity of the material. Increasing the number of walls enhance strength. Sparse wall density saves material, sacrifice for strength. Layer thickness enhances the printing quality and printing time. The parameter like bed temperature, orientation and printing speed will be made constant. The reinforced metallic wire will be of diameter 1.2mm.

3.5.1 Testing using UTM

A Universal tensile material testing system (MTS) was used to test the 3D-printed parts. Crosshead speed was maintained at 2 mm/min, a typical speed for 3D-printed parts. The experiment setup consists of MTS equipment, a specimen holder, and a strain gauge to calculate the elongation of the specimen. The data we take includes tensile strength, compressive strength, modulus of elasticity, and elongation at break for specimen. Initially we tested, the tensile strength of the 3D printed PLA+ as shown in the figure 3.7 and then we tested compressive strength of it figure 3.8.

Figure 3.7: Tensile Testing in UTM

Figure 3.8: Compression Testing in UTM

3.6 Vibration Test

Vibration test, used to evaluate the performance during dynamic loading. This test is done to evaluate the structural response during impact loading.

3.6.1 Preparation of 3D Samples

The vibration test samples, prepared according to ASTM D4566 method aims to determine the vibration damping of the PLA+ specimen under different printing pattern rectilinear, gyroid and honey comb pattern. Each specimen measured 100 mm in length, 100 mm in width and 4 mm in thickness, designed specifically for impact vibration analysis.

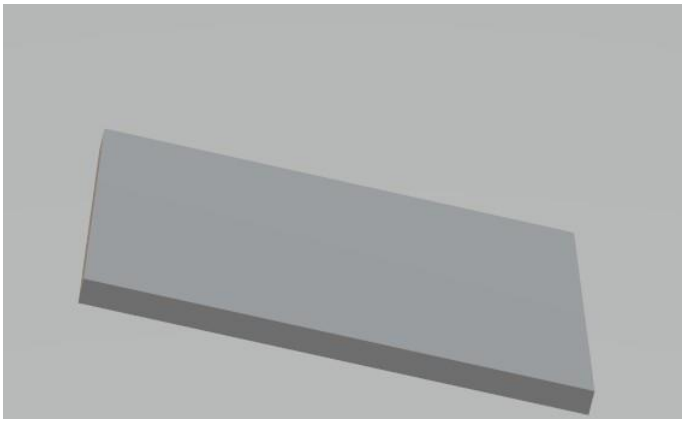

Figure 3.9: Impact Test specimen

3.6.2 Experimental Setup

The experimental setup consists of a specimen suspended by fixed strings, with an impact weight (a nut) 20gm dropped from a height of approximately 25 cm. Upon impact, the system undergoes vibration, and the damping rate is measured using an MPU 6050 accelerometer. The setup is used to analyze the vibration response of specimens with different infill patterns, as illustrated in the figure.

Figure 3.10: Impact Test setup

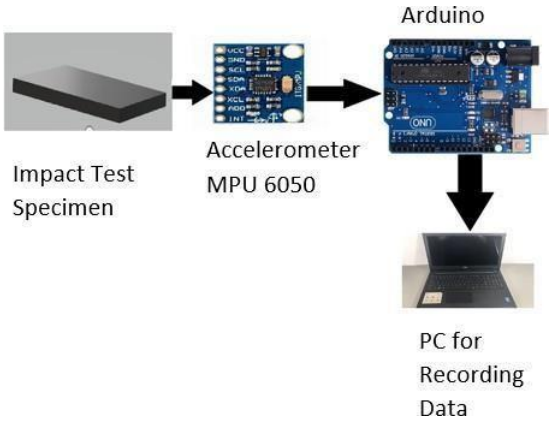

Figure 3.11: Impact Test workflow

CHAPTER 4:
RESULT AND DISCUSSION

4.1 Tensile Test

Tensile test of ASTM-D638-14 type I is conducted for 30 non-reinforced and 10 reinforced specimen.

4.1.1 Tensile test Data Collection

The figure below shows the result of tensile testing of the specimen.

Figure 4.1: Tensile test result

Figure 4.2: Tensile test result of wire-reinforced

Temp (°C)	Patt	Infill(%)	Peak L.	Disp	T-Streng(Mpa)	Y-Modulus
220	Rec.	60	3.3	6.4	70.51	11 GPA
200	Gyroid	30	3.25	6.3	69.49	9 GPA
220	Rec.	30	3.05	5.4	65.17	8 GPA
220	Rec.	80	2.75	5.7	58.76	8.22 GPA
220	Honey	90	3.00	5.4	64.1	3.18 GPA
220	Rec.	90	3.4	6.9	72.65	6.02 GPA
220	Rec.	90	2.35	7.4	50.21	5.68 GPA
220	Rec.	80	3.35	8.8	71.58	12 GPA
220	Rec.	90	3.35	8.8	71.58	12.3 GPA
230	Gyroid	30	2.9	6.7	61.97	8.45 GPA
230	Honey	30	2.9	5.7	61.97	9.87 GPA
230	Rec	30	2.4	10.0	51.28	18.5 GPA
230	Honey	60	3.15	6.9	67.3	9.17 GPA
230	Rec	60	2.85	6.8	60.94	10.1 GPA
230	Honey	90	3.05	4.4	65.17	16.4 GPA
230	Gyroid	90	3.3	8.1	70.51	20 GPA
230	Rec.	90	3.05	10.4	65.17	7.34 GPA
200	Rec.	30	3.25	6.2	69.49	7 GPA
230	Rec.	80	3.72	8.7	79.49	8.5 GPA
200	Gyroid	90	2.1	1.4	44.87	10.9 GPA
200	Honey	30	1.85	1.5	39.53	8.33 GPA
200	Honey	30	2.85	7.4	60.94	9.51 GPA
220	Gyroid	85	2.5	4.3	53.42	5.94 GPA
220	Gyroid	94	3.0	3.5	64.1	12.1 GPA
220	Gyroid	60	3.4	9.7	72.65	4.7 GPA
220	Gyroid	97	3.65	8.7	78.08	14.1 GPA
220	Honey	60	3.45	8.5	73.72	11.3 GPA
220	Rec.	30	3.5	8.7	74.79	9.17 GPA
220	Rec.	90	3.9	8.2	83.33	7.8 GPA
220	Honey	30	3.05	5.8	65.17	11.9 GPA

Table 4.1: Experimental results of 3D printed non-reinforced sample under varying printing parameters.

Specimen	Fill	P-Load (KN)	Disp(mm)	T-Strength)	Y-modulus(GPA)
Reinforced 1-wire	60	3.6	7.6	76.92	12.9
Reinforced 1-wire	90	3.35	6.2	71.58	7.49
Reinforced 1-wire	30	2.85	7.0	60.94	9.2
Reinforced 3-wire	80	2.55	7.2	54.49	16.4
Reinforced 3-wire	90	2.6	5.7	55.56	19.4
Reinforced 3-wire	30	2.7	9.1	57.69	14.6
Reinforced 2-wire	30	2.75	3.4	58.7	13.3
Reinforced 3-wire	60	2.85	8.3	60.94	7.65
Reinforced 3-wire	80	3.25	6.0	69.49	11.8
Reinforced 2-wire	80	3	1.0	64.1	8.33

Table 4.2: Mechanical properties of reinforced specimens with different reinforcement configurations.

Below, We have provided the comparison for the peak load of each of the specimen including, reinforced and non-reinforced.

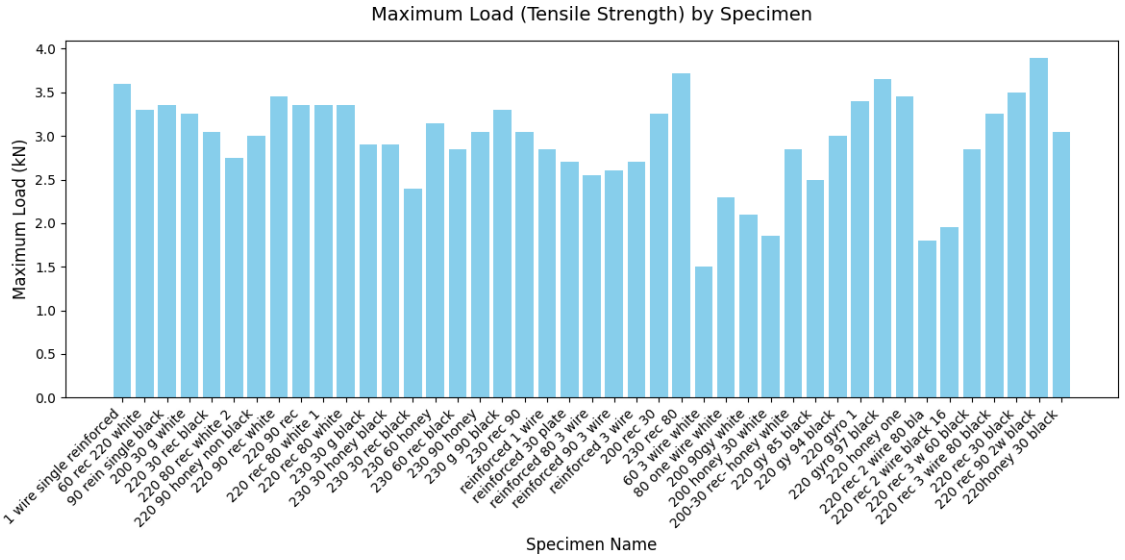

Figure 4.3: Result of Breaking point for three wire reinforced PLA+

4.1.2 Effect of Parameter on the Tensile Strength(Peak Load) in non-reinforced specimen

Below, We have provided how Temperature and Density correlate with the Peak Load /Tensile strength, average peak load by pattern, average peak load by temperature, av-

erage peak load by infill density.

Pearson Correlation Matrix

	Temperature(C)	Density	Peak Load(KN)
Temperature	1.000000	0.262312	0.262931
Density	0.262312	1.000000	0.174996
Peak Load	0.262931	0.174996	1.000000

Table 4.3: Pearson Correlation Matrix

Correlation between Temperature and Peak Load: Pearson correlation coefficient: 0.263 P-value: 0.160 and Correlation between Density and Peak Load: Pearson correlation coefficient: 0.175, P-value: 0.355

Average Peak Load by Pattern

We saw that average peak load bear by rectilinear pattern is higher comparative to the gyroid and honeycomb.

Pattern	Average Peak Load(KN)
Gyroid	3.025000
Honey	2.912500
Rec	3.162143

Table 4.4: Average Peak Load for Different Patterns

Average Peak Load by Temperature

We saw that nozzle printing temperature of 220 degree celcius give higher peak load compared to the 200 and 230 nozzle printing temperature.

Temperature	Average Peak Load(KN)
200	2.680000
220	3.190625
230	3.035556

Table 4.5: Average Peak Load by Temperature

Average Peak Load by Density

Following data listed in the table can be summarized:

Infill Density(%)	Average Peak Load(KN)
30	2.91
60	3.23
80	3.273
90	3.28
94	3.3

Table 4.6: Average Peak Load by Density

Observation

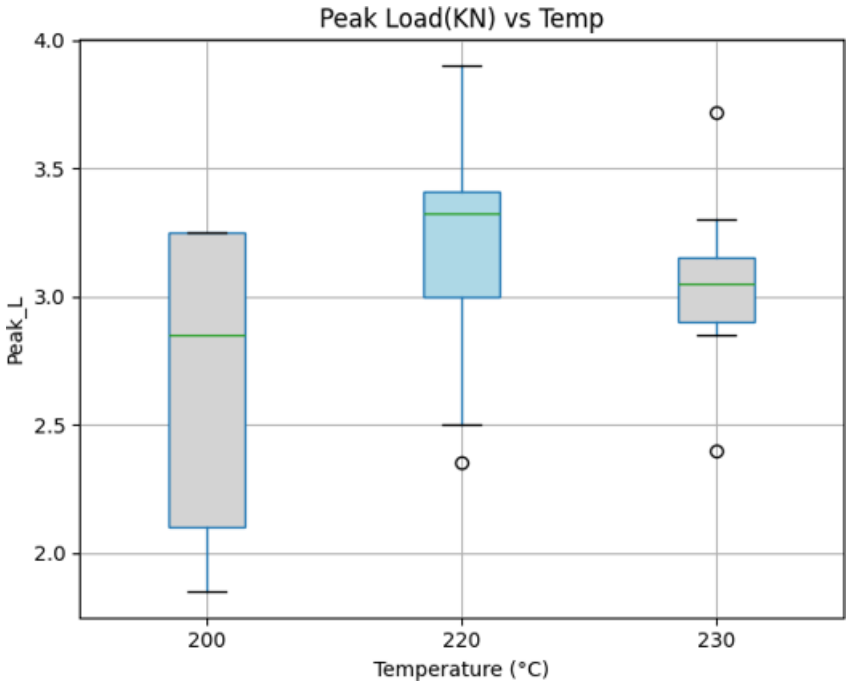

Figure 4.4: Box Plot for Temperature vs Peak Load for PLA+

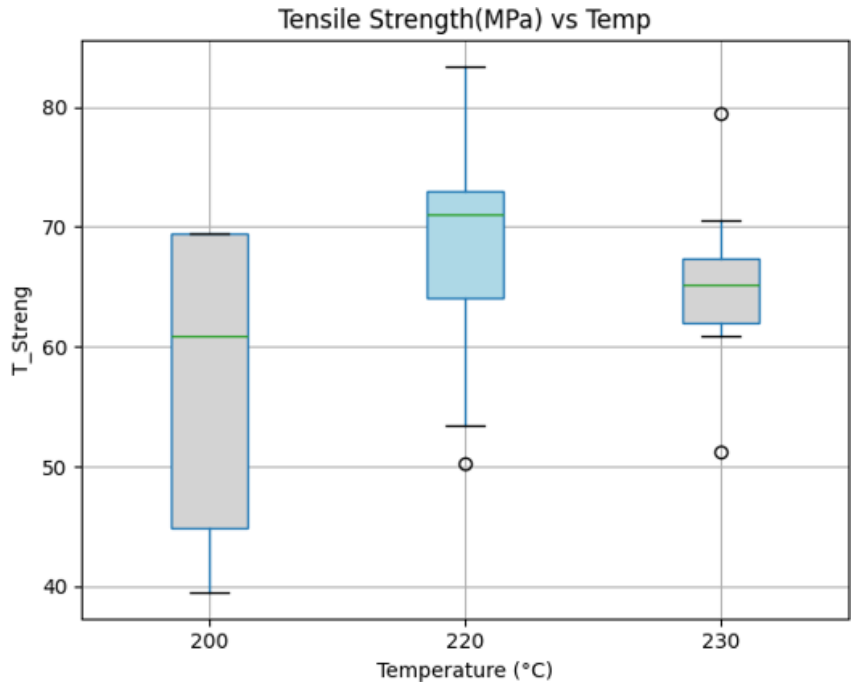

Figure 4.5: Box Plot for Temperature vs Tensile Strength for non-reinforced PLA+

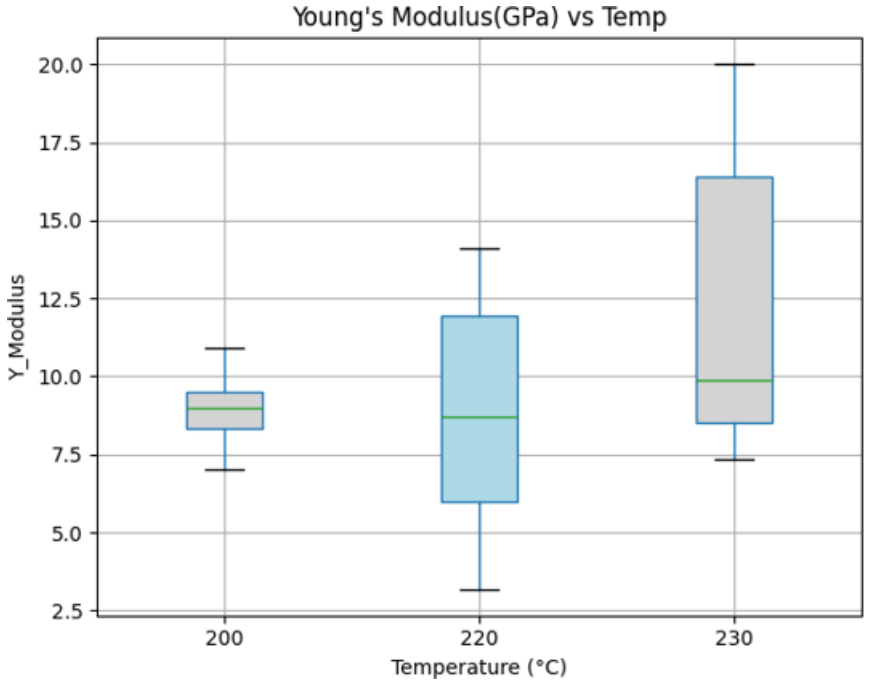

Figure 4.6: Box Plot for Temperature vs Young Modulus for non-reinforced PLA+

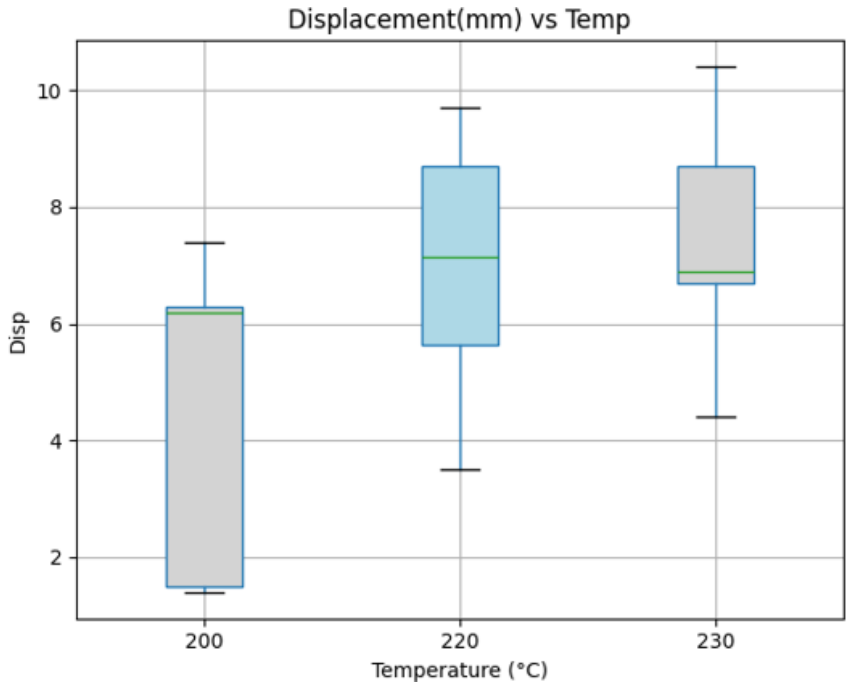

Figure 4.7: Box Plot for Temperature vs Desplacement for non-reinforced PLA+

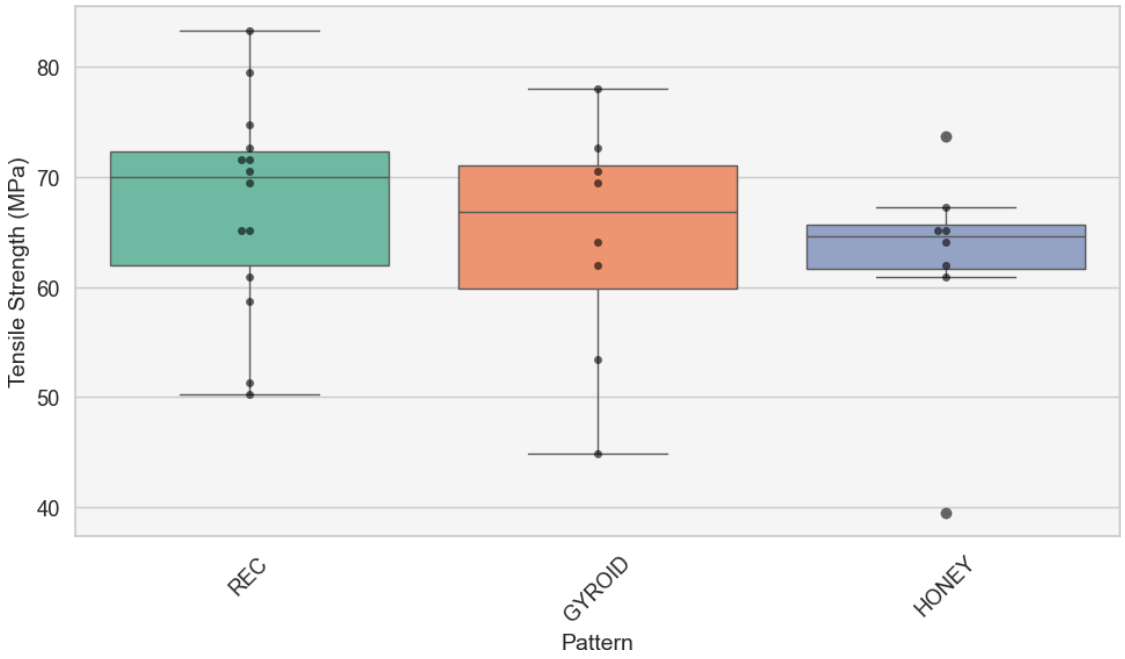

Figure 4.8: Box Plot for Tensile Strength for different printing pattern in non-reinforced PLA+

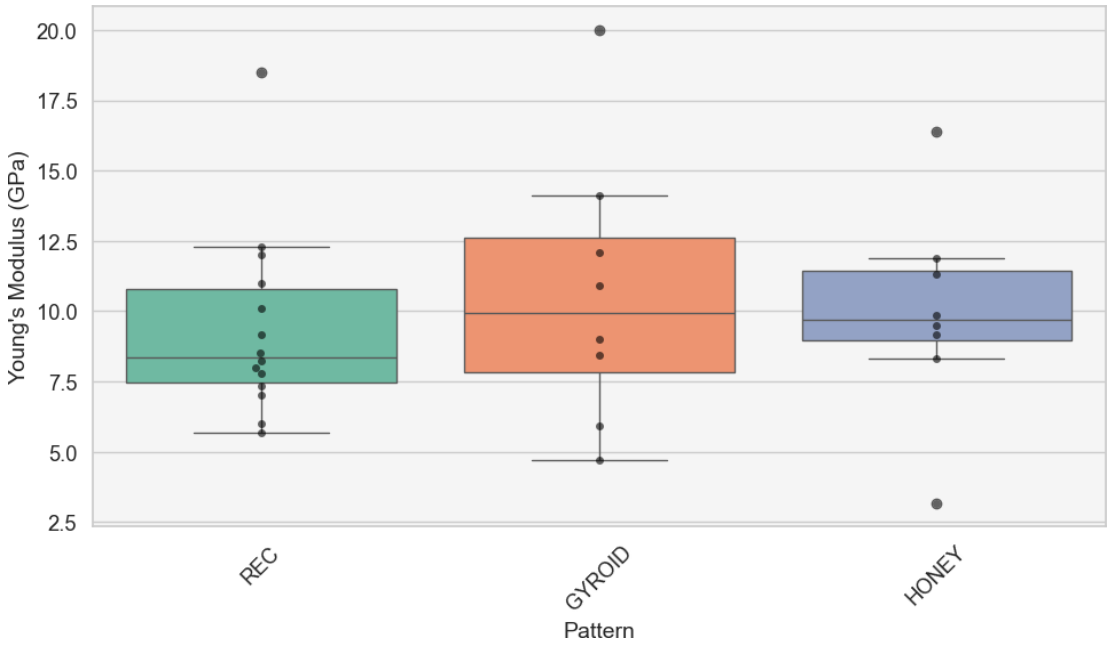

Figure 4.9: Young modulus distribution by pattern in non-reinforced PLA+

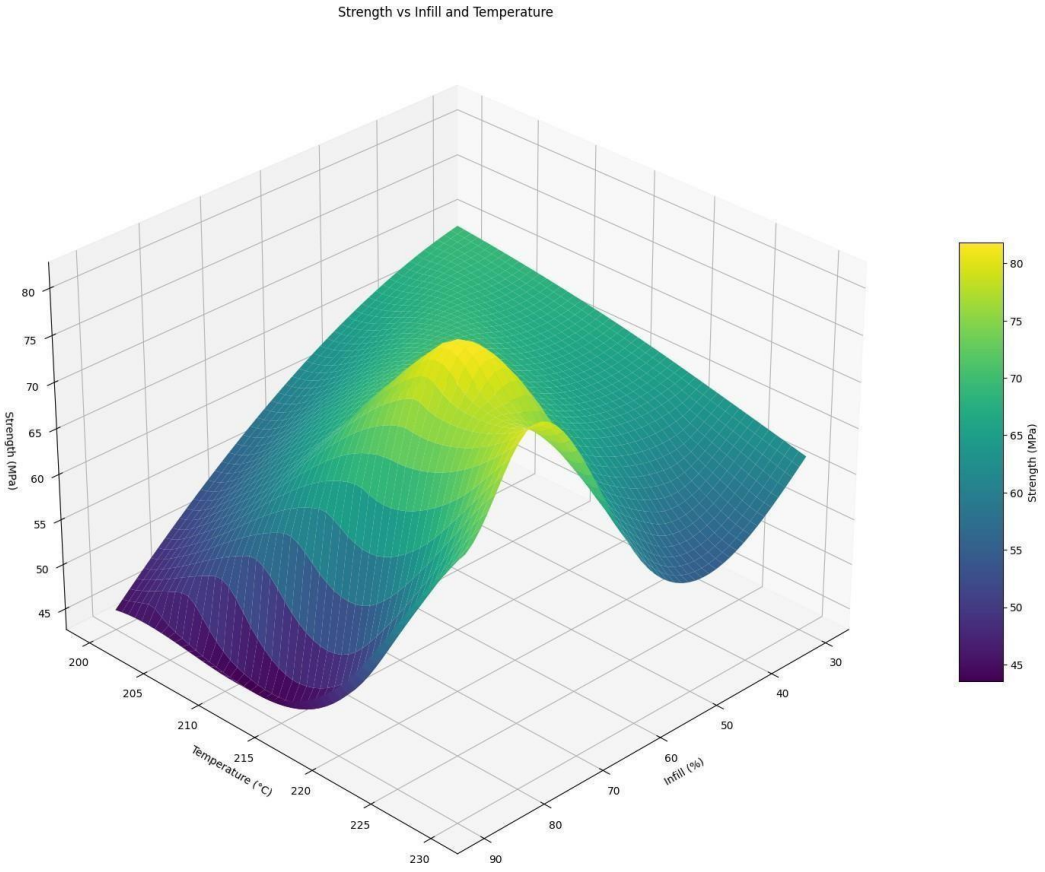

Figure 4.10: Surface plot of temperature, density and tensile strength for non-reinforced PLA+

We observed that rectilinear show higher tensile strength compared with gyroid and honeycomb while nozzle temperature of 220 is best for tensile strength. And, As infill density is increased, The ultimate tensile strength also increases but the rate at which strength can be increase is gradually decreased as infill density increased. so, Infill density of 80 and around is best for the tensile strength.

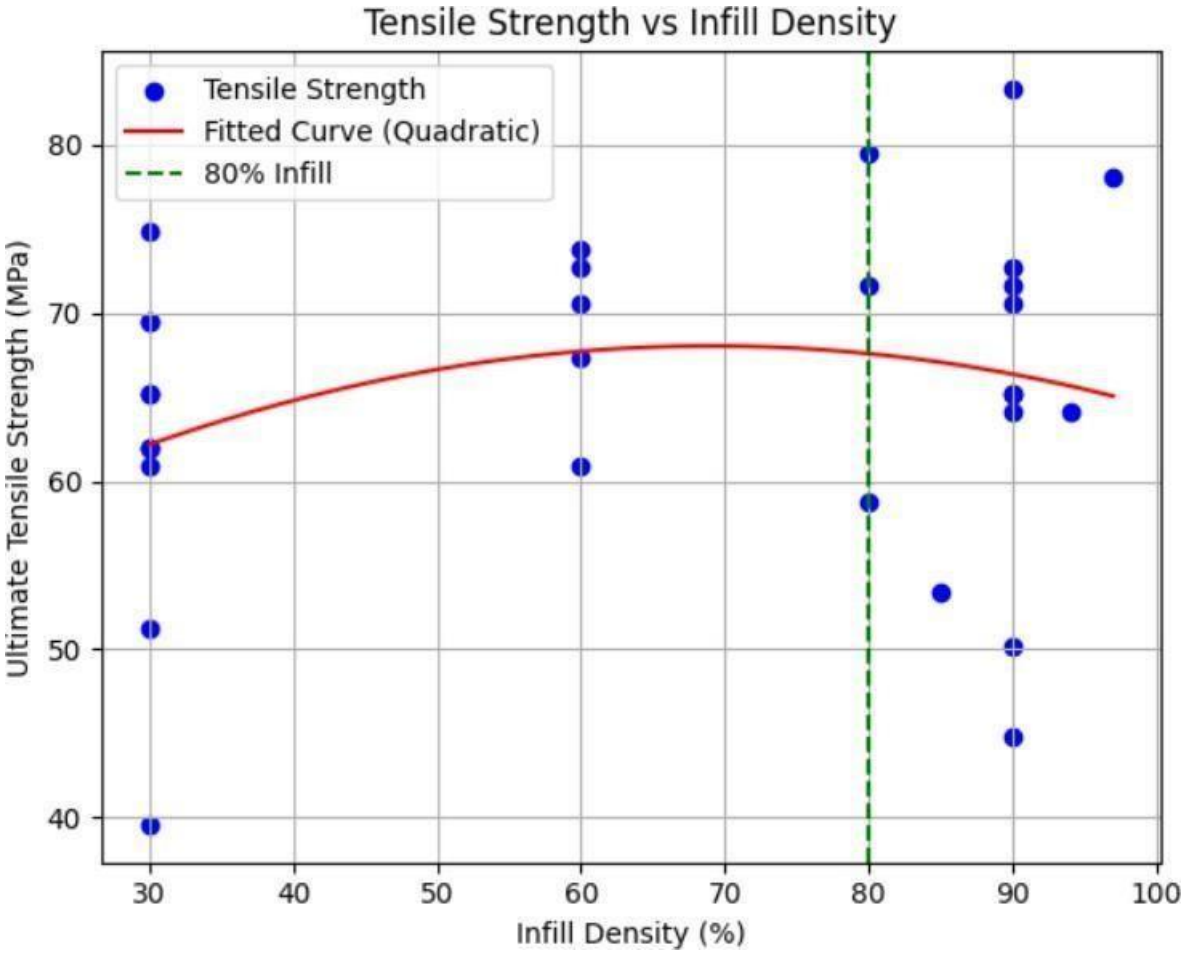

Figure 4.11: Tensile Strength vs Infill Density for PLA+

Some obervation regarding stiffness(young modulus) is provided below:

- Temperature Effect: A modest temperature increase from 200°C to 220°C can enhance modulus for some patterns (e.g., ”rec”), but the effect is pattern-dependent and not universally beneficial.
- Pattern Selection: ”Gyroid” appears to provide the best stiffness at high densities, while ”honey” shows the most variability, possibly due to its complex geometry affecting load distribution.

4.1.3 Analysis using Supervised Learning

Regression Analysis

Following result was seen doing the regression analysis:

Model	0LS(Ordinary Least Square)
R-squared	0.113
Mean Absolute Error	0.353

Table 4.7: Result for Regression Analysis

Random Forest

Following result was seen doing the Random Forest analysis:

R-squared (Test Set)	-1.730
Mean Squared Error (Test Set)	0.115

Table 4.8: Result from Random Forest

Polynomial Regression

Following result was seen from Polynomial Regression:

R-squared (Test Set)	-9.066
Mean Squared Error (Test Set)	0.425

Table 4.9: Result from Polynomial Regression

Gradient Boosting Regression

Following result was seen from Gradient Boosting Regression:

R-squared (Test Set)	-2.057
Mean Squared Error (Test Set)	0.129

Table 4.10: Result from Gradient Boosting

Discussion

Comparing all the analyses, we saw that the value of Mean Squared error(MSE) is low for random forest comparatively. since, MSE measures the average squared difference between the actual values and the predicted values. It helps assess how well a regression model fits the data. We can use random forest to estimate the strength of some the materials to be printed:

4.1.4 Prediction using Regression Analysis

Output from regression Analysis prediction:

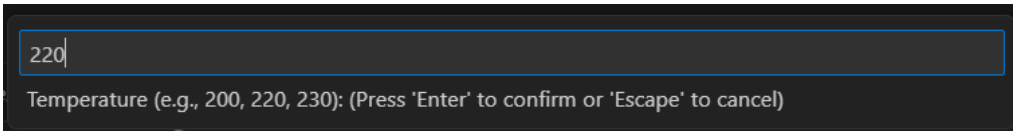

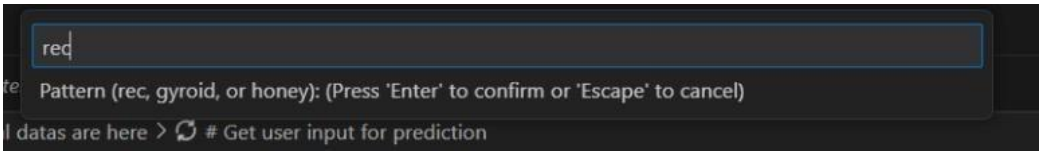

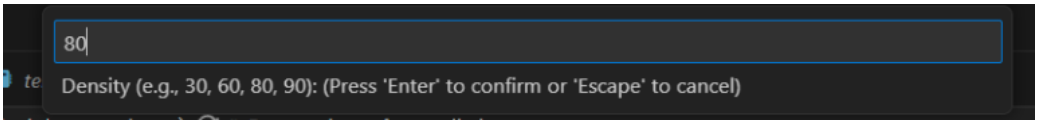


```
Enter values to predict Peak Load:

Predicted Peak Load: 3.064
Exiting prediction mode.
```

Discussion

We see that, the predicted tensile strength show the mean absolute error of 0.115 which could be improved by increasing number of test specimen and addressing further issue like use of clamp which possibly may cause the necking problem leading to the outlier of the data.

4.1.5 Tensile Test for Reinforced materials

Interpretation of data of reinforced specimen is done below:

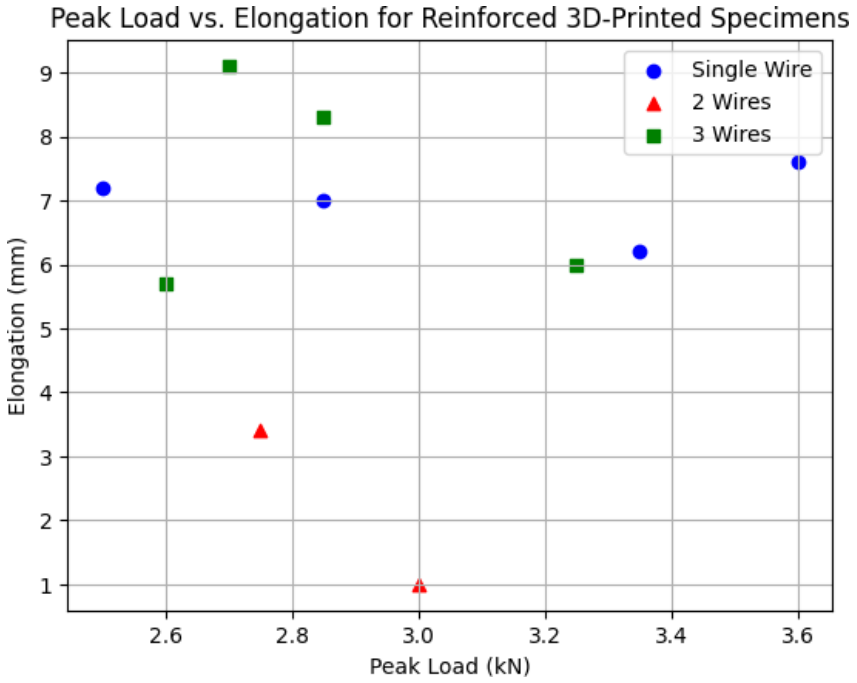

Interpretation of the Scatter Plot

- **Single Wire**: Points will cluster around 2.5–3.6 kN and 6.2–7.6 mm, showing moderate peak load and elongation.
- **2 Wires**: Points will be lower on both axes (2.75–3 kN, 1–3.4 mm), indicating poor performance in both peak load and elongation.
- **3 Wires**: Points will show higher elongation (5.7–9.1 mm) and peak load (2.6–3.25 kN), with a wider spread, especially at 30% density.

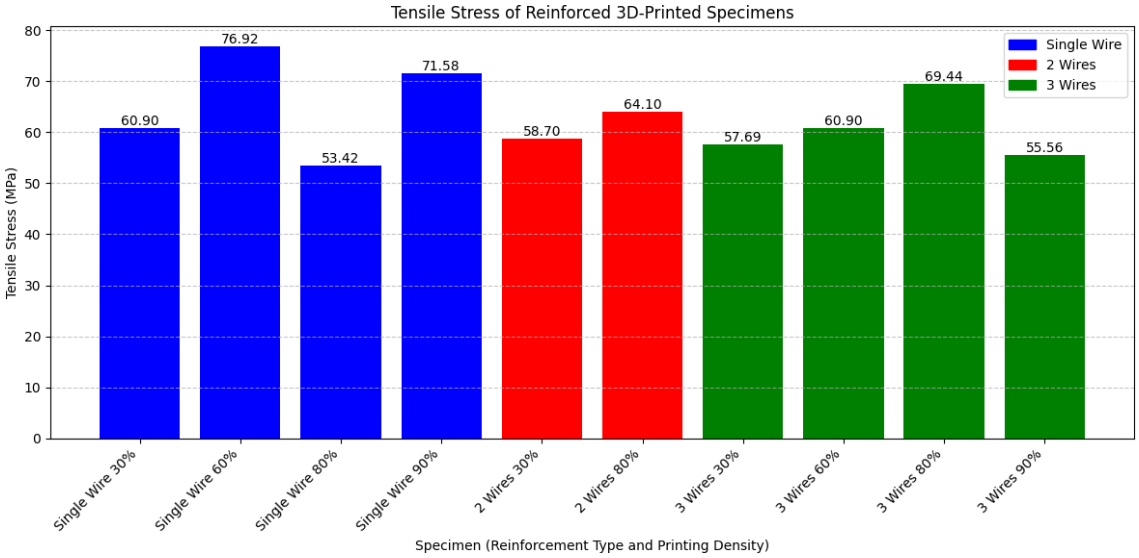

Figure 4.12: Bar graph for Tensile stress of Reinforced specimen for reinforced PLA+

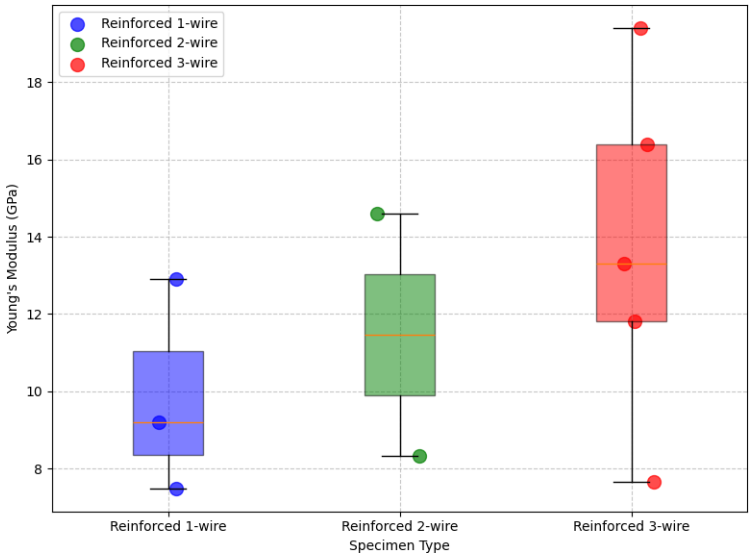

Figure 4.13: Box Plot for Young Modulus vs specimen type for reinforced PLA+

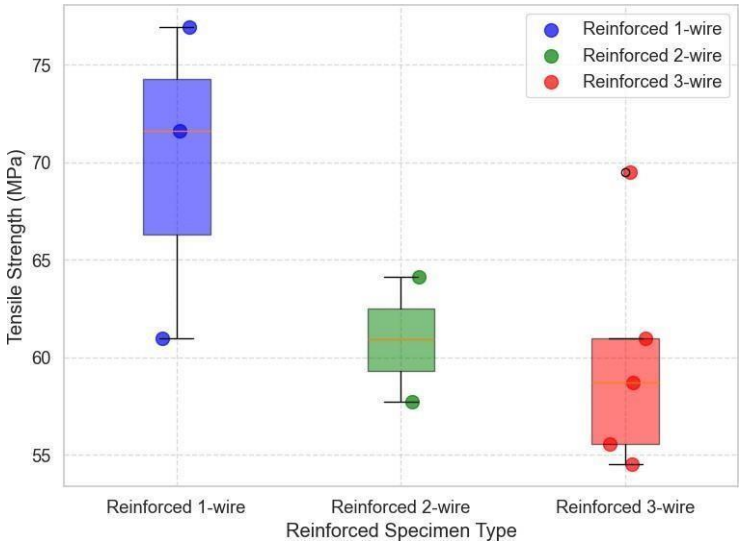

Figure 4.14: Box Plot for Tensile Strength vs specimen type for reinforced PLA+

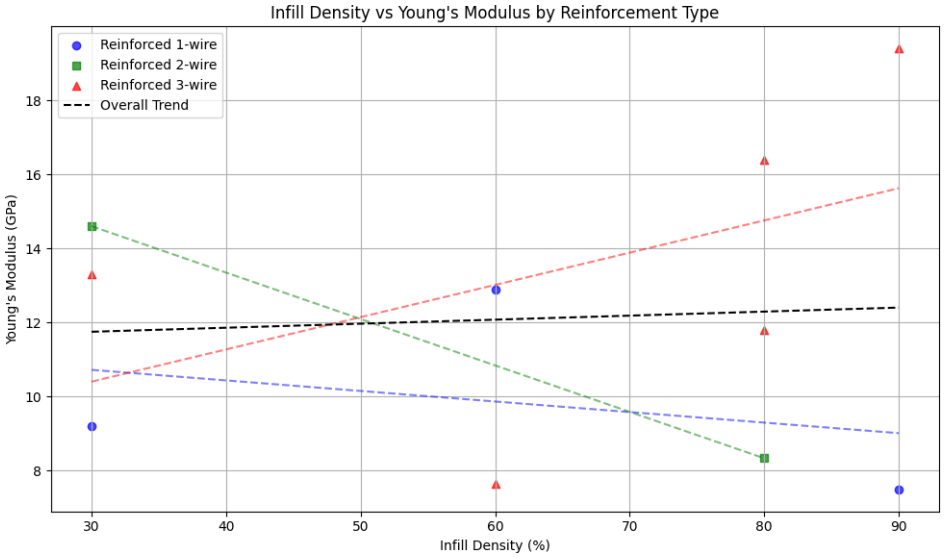

Figure 4.15: Scatter plot with trend lines for Young's modulus vs infill density for reinforced PLA+

Discussion

We find out that single wire reinforced specimen gave higher tensile strength compared to double and triple wire reinforcement.This is due to the space required to reinforce wire is significantly increased as number of wire is increased. This reduce the overall strength of the specimen. So, we concluded that reinforcing a small volume of the material helps to increase the strength of material while adding more will reduce in return. This could be improved by reinforcing using the machine, which could reduce

the gap needed to reinforce. Further using epoxy resin as the adhesive manually caused printing quality to deteriorate which could be reduced by using printer that could be used using adhesive materials too. For stiffness, Some observations are provided below:

- Optimal Reinforcement: The 3-wire configuration at 80%–90% infill yields the highest Young's modulus (16.4 GPa), making it the most effective reinforcement strategy for maximizing stiffness.
- Wire Number Impact: Increasing from 1 wire (7.49–12.9 GPa) to 3 wires (11.8–16.4 GPa) significantly boosts stiffness, with 2 wires (8.33 GPa) showing an intermediate effect.
- Application Suitability: Reinforced samples with 3 wires at 80%–90% infill are suitable for applications needing high stiffness (e.g., structural components), while single-wire at 60% could suffice for lighter-duty uses.

4.1.6 Analysis Using Simulation

For the simulation we use explicit dynamics in Ansys. Explicit dynamics is a time integration method used to perform dynamic analyses where speed is important. It is computationally efficient for the analysis of large models with relatively short dynamic response times and for the analysis of extremely discontinuous events or processes. For processing we defined connection type is Reinforced and mesh was generated.

Non-Reinforced PLA+

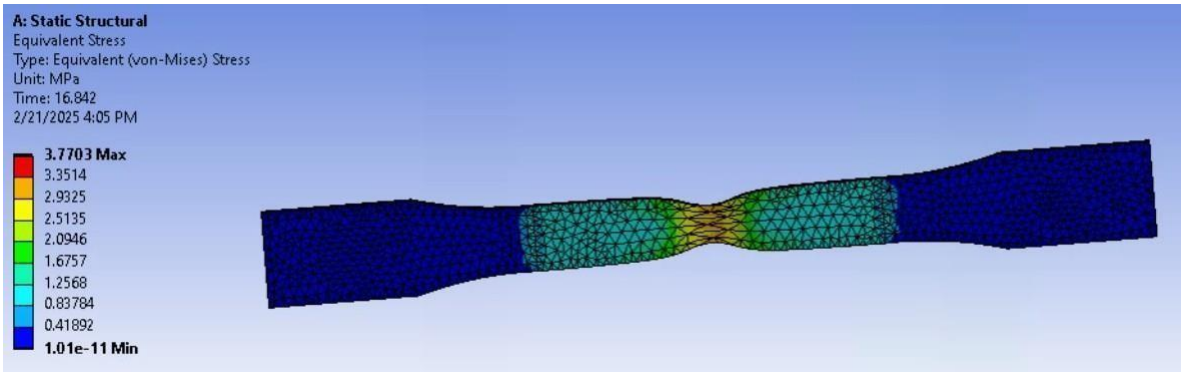

Figure 4.16: Result of Breaking point for non-reinforced PLA+

Single wire reinforced PLA+

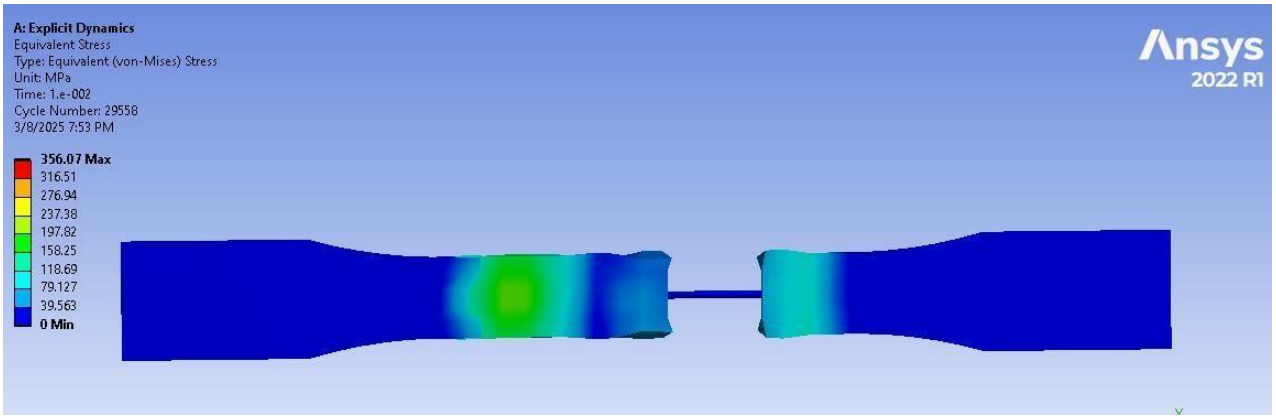

Figure 4.17: Result of Single Wire reinforced PLA+

Double Wire reinforced PLA+

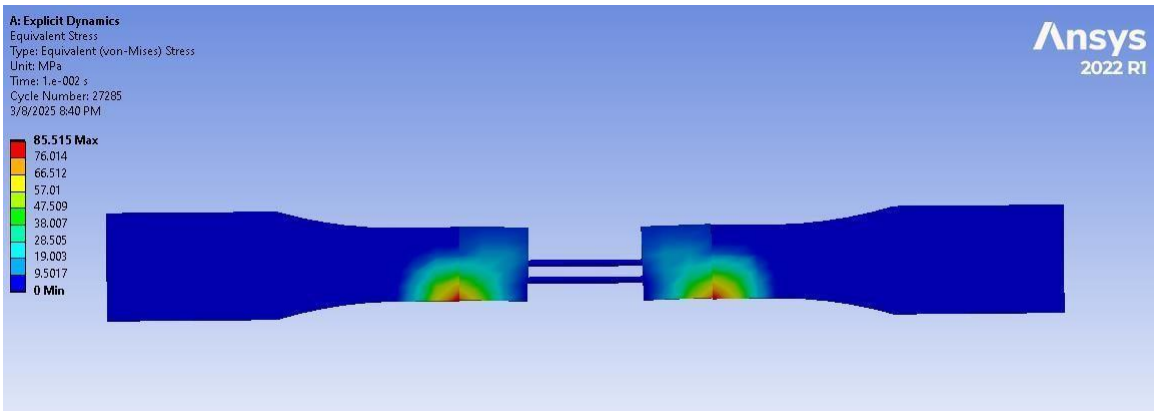

Figure 4.18: Result of Breaking point for two wire reinforced PLA+

Triple Wire reinforced PLA+

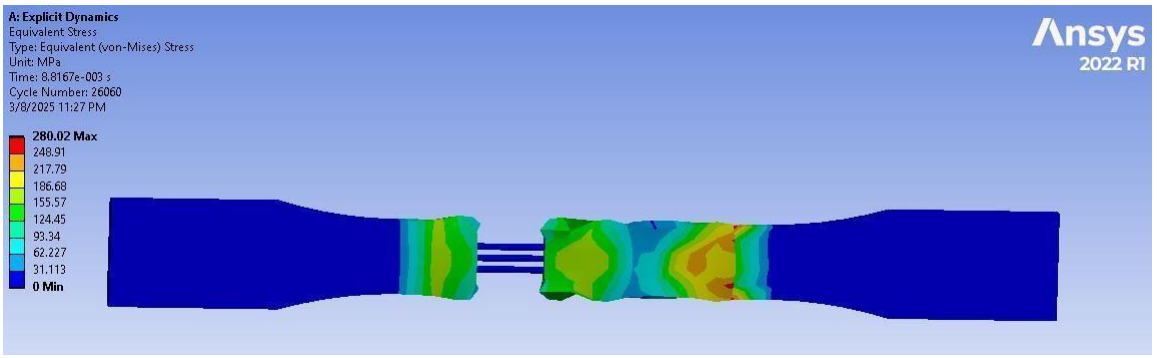

Figure 4.19: Result of Breaking point for three wire reinforced PLA+

Related Discussion

The experimental and numerical analysis of ASTM D638 specimens revealed that reinforcement with single, double, and triple mild steel wires enhanced their mechanical properties and altered their failure behavior. The non-reinforced specimen exhibited a brittle fracture at the central region, consistent with its inherent brittleness, which was accurately replicated in ANSYS simulations. With single-wire reinforcement, failure became more ductile as the wire delayed crack propagation, a trend also observed in simulations. The strong correlation between experimental and simulation results validates ANSYS as a reliable tool for predicting tensile failure in reinforced polymer composites.

4.2 Compression Test

The compression specimen was prepared at nozzle temperature 220 degree celsius, Rectilinear as infill pattern and infill density 30%, 60%, 80% and 90%. Below weight of specimen for each infill density is provided to compare tensile strength per weight:

Density (%)	Weight (grams)
30	21.09
60	34.66
80	43.76
90	48.36

Table 4.11: Weight values for different infill densities

The result and analysis of the data obtained is provided below:

4.2.1 Result of compression test

The figure below shows the result of final specimen after compression test:

Figure 4.20: Compression Test

4.2.2 Data Output and Discussion

Graph showing Load versus Displacement

Below is the graph comparing how Load vs Displacement is observed for specimen with different infill density.

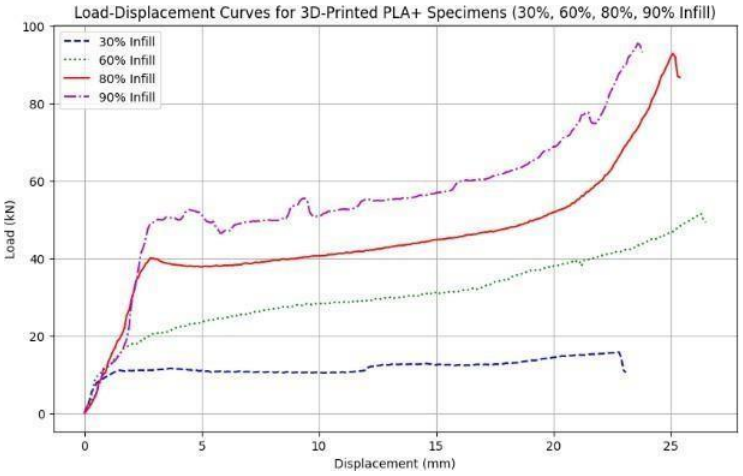

Figure 4.21: Load vs Displacement Curve

Infill(%)	Max.Load(kN)	Disp.at Max.Load(mm)	Max-Strength(MPa)	Fail.Point(mm)
30	15.75	22.8	3.45	21.3
60	51.5	26.3	11.28	26.4
80	92.85	25.1	20.34	25.2
90	95.5	23.6	20.93	23.7

Table 4.12: Compressive Test Results for Different Infill Densities

Infill Density (%)	**Max Tensile Strength per Weight**
30	0.16
60	0.325
80	0.46
90	0.43

Table 4.13: Max tensile strength per weight for different infill densities

4.2.3 Observations

Compressive strength increases significantly with higher infill densities: 3.45 MPa (30%) → 11.28 MPa (60%) → 20.34 MPa (80%) → 20.93 MPa (90%). The largest relative increase occurs between 30% and 60% ($\tilde{3}.27$x), with smaller gains from 60% to 80% ($\tilde{1}.80$x) and 80% to 90% ($\tilde{1}.02$x), suggesting diminishing returns at very high infill densities. Displacement at maximum load increases from 22.8 mm (30%) to 26.3 mm (60%) but decreases to 25.1 mm (80%), and 23.6 mm (90%). This suggests that while 80% and 90% infill provide the highest strength, it may result in a slightly less ductile or more brittle behavior, leading to failure at a lower displacement compared to 60%. For maximum compressive strength, 90% infill is the best, offering 20.93 MPa. However, the marginal gain from 80% (20.34 MPa) to 90% (21.89 MPa) is only $\tilde{7}$.6%, which may not justify the additional material use and print time for some applications. If ductility or deformation capacity is a priority, 60% infill might be preferable, as they sustain higher displacements before failure.

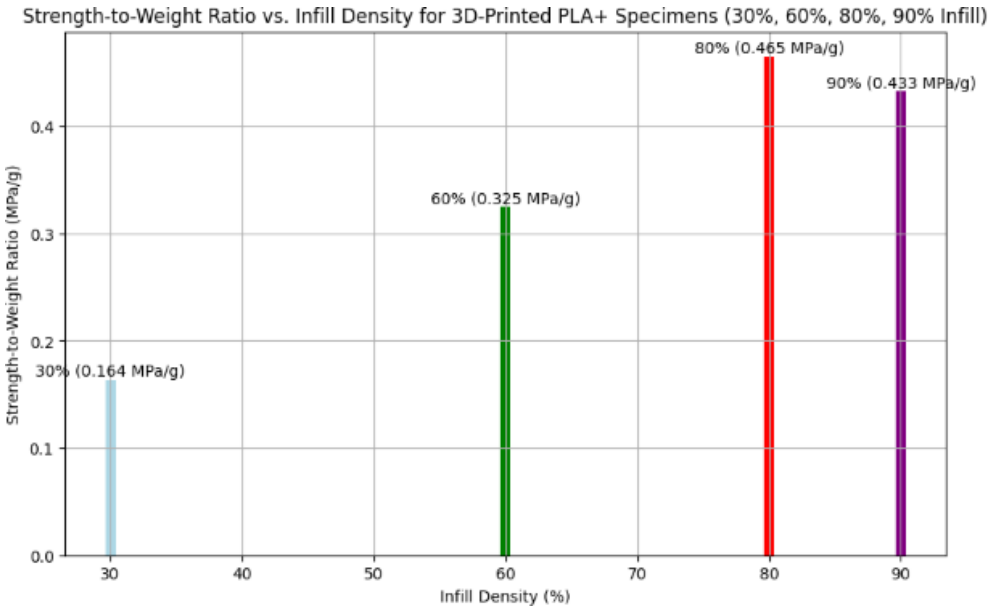

Figure 4.22: Strength to weight ratio at Different infill

The strength-to-weight ratio increases from 0.164 MPa/g (30%) to 0.465 MPa/g (80%), then decreases slightly to 0.433 MPa/g (90%). The 80% infill offers the highest efficiency (0.465 MPa/g), making it the most material-efficient choice in terms of strength per gram of material. The 90% infill, while providing the highest compressive strength (20.93 MPa), is less efficient (0.433 MPa/g) due to the additional 4.6 g of weight for only a 0.59 MPa gain in strength.

4.2.4 Discussion

Overall Trend

Increasing infill density from 30% to 90% significantly enhances the compressive strength of 3D-printed PLA+ specimens with a rectilinear infill pattern. The strength increases from 3.45 MPa (30%) to 20.93 MPa (90%), reflecting the greater material density and load distribution provided by higher infill.

Optimal Infill for Strength

90% infill provides the highest compressive strength (20.93 MPa), making it ideal for applications requiring maximum load-bearing capacity under compression.

Tradeoffs

However, 90% infill results in slightly lower displacement at failure (23.7mm) compared to 60% (26.4 mm) and 80% (25.2 mm), suggesting it may be less ductile or more prone to brittle failure. For applications where deformation capacity or material efficiency is important, 80% infill (20.35 MPa) might be a more practical choice, as it offers nearly comparable strength with potentially better material usage.

- The 30% infill has the lowest efficiency (0.164 MPa/g), indicating poor material use for strength, making it unsuitable for load-bearing applications.
- The 80% infill strikes an optimal balance, offering high strength (20.34 MPa) and the best efficiency (0.465 MPa/g), with a failure/decrease point of 25.2 mm, suggesting good ductility.

4.3 Vibration Analysis

Data collected for each test and its analysis and conclusion is provided below:

4.3.1 Data Summary (Damping rates,1/s)

Structure	Test 1	Test 2	Test 3	Test 4	Test 5	Test 6
Rectilinear	10.28	10.76	6.79	9.63	5.57	6.68
Honeycomb	6.08	5.65	7.53	7.89	5.29	6.25
Gyroid	6.15	6.27	6.34	6.79	6.94	6.40

Table 4.14: Damping Rates (1/s) for Different Structures

4.3.2 Calculations

Rectilinear damping:

$$\text{Mean} = \frac{10.28 + 10.76 + 6.79 + 9.63 + 5.57 + 6.68}{6} = \frac{49.71}{6} = 8.29/\text{s}$$

Standard Deviation (σ):

$$\text{Deviations: } [1.99,\ 2.47,\ -1.50,\ 1.34,\ -2.72,\ -1.61]$$

$$\text{Squared deviations: } [3.96,\ 6.10,\ 2.25,\ 1.80,\ 7.40,\ 2.59]$$

$$\text{Variance} = \frac{24.10}{6} = 4.02$$

$$\sigma = \sqrt{4.02} = 2.00/\text{s}$$

$$\text{Range} = 5.57 \text{ to } 10.76 \quad (5.19/\text{s})$$

Honey Comb damping:

$$\text{Mean} = \frac{6.08 + 5.65 + 7.53 + 7.80 + 5.29 + 6.25}{6} = \frac{38.69}{6} = 6.45/\text{s}$$

Standard Deviation (σ):

$$\text{Deviations: } [-0.37,\ -0.80,\ 1.08,\ 1.44,\ -1.16,\ -0.20]$$

$$\text{Squared deviations: } [0.14,\ 0.64,\ 1.17,\ 2.07,\ 1.35,\ 0.04]$$

$$\text{Variance} = \frac{5.41}{6} = 0.90$$

$$\sigma = \sqrt{0.90} = 0.95/\text{s}$$

$$\text{Range} = 5.29 \text{ to } 7.89 \quad (2.60/\text{s})$$

Gyroid damping:

$$\text{Mean} = \frac{6.15 + 6.27 + 6.34 + 6.79 + 6.94 + 6.40}{6} = \frac{38.89}{6} = 6.48/\text{s}$$

Standard Deviation (σ):

$$\text{Deviations: } [-0.33,\ -0.21,\ -0.14,\ 0.31,\ 0.46,\ -0.08]$$

$$\text{Squared deviations: } [0.11,\ 0.04,\ 0.02,\ 0.10,\ 0.21,\ 0.01]$$

$$\text{Variance} = \frac{0.49}{6} = 0.08$$

$$\sigma = \sqrt{0.08} = 0.29/\text{s}$$

$$\text{Range} = 6.15 \text{ to } 6.94 \quad (0.79/\text{s})$$

4.3.3 Discussion

The rectilinear pattern dampens vibrations the fastest, with a rate of 8.29 /s due to its strong directional rigidity. However, its performance is inconsistent (σ = 2.00 /s) due to inherent weak axes. The honeycomb structure, on the other hand, offers a more balanced response, with a moderate damping rate of 6.45 /s and better consistency (σ = 0.95 /s), benefiting from its hexagonal symmetry and the ability to absorb energy efficiently. Meanwhile, the gyroid pattern maintains a stable damping rate of 6.48/s with minimal variation (σ = 0.29 /s), a result of its complex isotropic nature. However, its decay is slightly slower, possibly due to internal resonance effects.

4.4 Limitations

- The interface between the clamp and the specimen introduced shear stress, which may potentially affect the accuracy of the output data.
- Study of tensile strength is limited to the 3 parameters only.
- We focused on the parameters causing more impact due to time limitation due to which more comprehensive study could not be carried out.
- Limited data during the prediction model can cause over-fitting of the data.
- Compressive strength analysis is conducted on infill density only while there was other parameters like layer height and printing temperature that could impact significantly.
- Vibration damping test is limited to the printing temperature only.
- The UTM that we used has some offset and issue in its clamp due to which our specimens broke frequently.
- Force required should be applied manually during the test, so sudden high force is applied in many test hampering the quality of data.

4.5 Problem Faced

- Achieving consistency in 3D printing was a major challenge, particularly in ensuring uniform print quality and proper adhesion when incorporating steel wire reinforcements. Variations in extrusion, temperature fluctuations, and layer bonding affected the overall structural integrity of the samples. Additionally, maintaining precise dimensions was difficult, as minor inconsistencies in infill distribution and specimen geometry led to variations in mechanical test results. This lack of uniformity impacted the accuracy and reliability of the data collected.

- Necking was frequently seen due to use of clamp during testing.

- Another critical issue was the placement of steel wire reinforcements within the PLA+ matrix. Proper alignment was essential to achieve the intended strengthening effect, but positioning multiple wires at specific locations without displacement proved difficult. Any deviation in placement could alter the stress distribution and influence failure behavior. Furthermore, strict adherence to ASTM D638 and ASTM D695 testing standards added to the complexity, as ensuring identical testing conditions for all specimens required precise control over environmental and procedural factors.

- Discrepancies between simulated and experimental results also posed challenges. While ANSYS Explicit Dynamics provided theoretical insights, the actual mechanical performance of the specimens deviated from these predictions due to factors such as imperfect adhesion, residual stresses, and minor manufacturing defects. Additionally, the material response of both reinforced and non-reinforced specimens exhibited unexpected failure patterns, necessitating further investigation to understand the underlying causes. These challenges highlighted the intricate nature of 3D printing with reinforcements and emphasized the need for improved control over the fabrication and testing processes.

4.6 Budget analysis

The budget utilized for the overall project from start to finish is shown in the table:

Items	Quantity	Cost	Remarks
Mild steel wire 1.2mm	0.5kg	Rs 200	
Epoxy Adhesive	2 sets	Rs 550	
Vibration Sensor SW-420	1	Rs 150	
Arduino Uno	1	1200	
PLA+ Filament	3	Rs 10,000	
Specimen Holding Clamp	2 pairs	Rs 2000	
Nut and Bolt	15	Rs 300	
Miscellaneous		Rs 2000	
Total Cost		Rs 15,600	

Table 4.15: Budget Analysis table.

4.7 Work Scheduling (Gantt Chart)

The entire workflow and scheduling of the tasks is represented in the following Gantt chart.

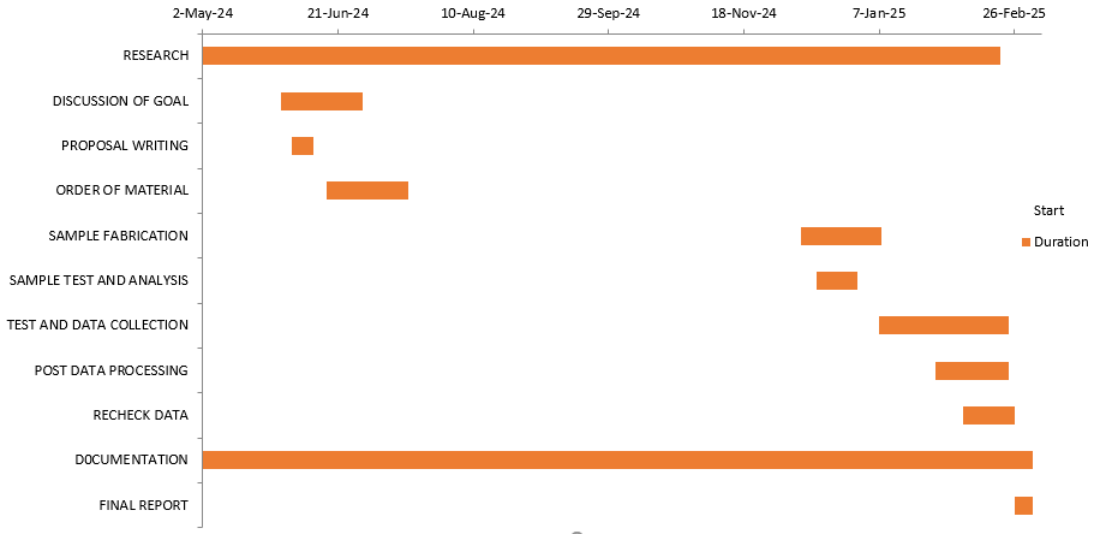

Figure 4.23: Gantt Chart

CHAPTER 5:
CONCLUSION AND FUTURE ENHANCEMENT

5.1 Conclusion

The study revealed that the rectilinear infill pattern exhibited the highest tensile strength compared to gyroid and honeycomb structures. This suggests that its linear alignment of material layers provides better load distribution and resistance to tensile forces. Among the tested printing temperatures, 220°C proved to be the most effective for tensile strength, as it facilitated stronger interlayer bonding and enhanced mechanical properties. Also, Increasing the infill density led to a significant improvement in tensile strength; however, the rate of increase gradually declined as density surpassed 80%. This diminishing return suggests that beyond a certain point, additional material contributes less to strength enhancement. The results indicate that 80% infill is an optimal choice, balancing material efficiency with structural integrity. While higher densities continue to improve strength, the tradeoff in print time and material usage may not always be justifiable. Young's modulus, representing stiffness, was found to be highest in the 220°C and in Gyroid pattern. Additionally, while a modest increase in temperature from 200°C to 220°C enhanced stiffness for certain patterns like rectilinear, the effect was not universally beneficial across all designs.

We obtained that the Mean Squared Error(MSE) was low for random forest. While Predicting tensile strength using random forest, we obtained absolute error of 0.115 which is in acceptable range. So, the prediction model is verified.

Wire reinforcement had a significant impact on tensile strength, with single-wire reinforcement outperforming double and triple-wire configurations. The increased spacing required for additional wires disrupted material continuity, weakening the structure. As a result, reinforcing a small volume of material proved more effective than excessive reinforcement. A potential improvement could involve precision-controlled reinforcement techniques to minimize gaps, possibly through automated methods or optimized adhesive application during printing. For stiffness, however, the three-wire reinforcement strategy at 80%–90% infill yielded the highest Young's modulus, reaching 16.4 GPa. This suggests that additional reinforcement enhances rigidity more effectively

than tensile strength. Interestingly, for single-wire reinforcement, 60% infill appeared to be optimal for stiffness, while higher densities resulted in reduced modulus, likely due to poor integration of reinforcing elements. These findings highlight that the ideal reinforcement strategy varies depending on whether strength or stiffness is the primary concern.

Compressive strength was significantly influenced by infill density, with higher densities yielding better load-bearing capacity. The compressive strength increased from 3.45 MPa at 30% infill to 20.93 MPa at 90%, confirming the trend that greater material density improves structural integrity under compression. However, beyond 80% infill, the increase in strength became marginal, with only a 7.6% improvement between 80% and 90%. This suggests that 80% infill strikes the best balance between strength, material efficiency, and print time.

Vibration damping characteristics varied significantly based on the infill pattern. The rectilinear pattern dampened vibrations the fastest due to its strong directional rigidity but showed inconsistent performance due to weak axes. The honeycomb pattern provided a more balanced response, efficiently absorbing energy through its hexagonal symmetry. Meanwhile, the gyroid pattern exhibited stable damping performance with minimal variation, likely benefiting from its isotropic structure. These findings suggest that selecting the optimal infill pattern depends on the specific mechanical properties required for an application, whether it be strength, stiffness, or energy absorption.

5.2 Scope for future enhancement

- Depth research on influence of other printing parameters on strength of PLA+ specimen could be conducted.
- Research could be done on the effect of different reinforcement patterns and materials.
- To study the effect of environmental factor on the mechanical performance.
- Using a reverse regression model, independent printing parameters can be used to predict the required strength of materials, saving materials and costs over the period of time.

- Other different test like shear, and flexural could be conducted.
- Reinforcing the metal in the 3D-printed specimen saves the cost of production and increases the overall strength of the specimen. So, Product could be manufactured by using reinforcement.

CHAPTER 6:
REFERENCES

1. Khosravani, M.R.; Reinicke, T. On the environmental impacts of 3D printing technology. Appl. Mater. Today 2020, 20, 100689.

2. Shaqour, B.; Abuabiah, M.; Abdel-Fattah, S.; Juaidi, A.; Abdallah, R.; Abuzaina, W.; Qarout, M.; Verleije, B.; Cos, P. Gaining a better understanding of the extrusion process in fused filament fabrication 3D printing: A review. Int. J. Adv. Manuf. Technol. 2021, 114, 1279–12

3. Radadiya, V. A., and Gandhi, A. H. (2022). A Study of Tensile Characteristics for Glass and Carbon Fiber Along with Sandwiched Reinforced ABS Composites. Journal of the Institution of Engineers (India)SeriesC(IEIC),103(5),1049–1057. https://doi.org/10.1007/s40032-022-00848-2

4. Khan, M. F., Alam, A., Siddiqui, M. A., Alam, M. S., Rafat, Y., Salik, N., and Al-Saidan, I. (2021). Real-time defect detection in 3D printing using machine learning. Materials Today: Proceedings, 42, 521–528. https://doi.org/10.1016/j.matpr.2020.10.482

5. Gebisa, A. W., and Lemu, H. G. (2019). Influence of 3D Printing FDM Process Parameters on Tensile Property of ULTEM 9085. Procedia Manufacturing,30,331–338. https://doi.org/10.1016/j.promfg.2019.02.047

6. Rodr´ıguez-Panes, A., Claver, J., and Camacho, A. M. (2018). The Influence of Manufacturing Parameters on the Mechanical Behaviour of PLA and ABS Pieces Manufactured by FDM: A Comparative Analysis. Materials, 11(8), 1333. https://doi.org/10.3390/ma 11081333

7. Maulud, D., and Abdulazeez, A. M. (2020). A Review on Linear Regression Comprehensive in Machine Learning. Journal of Applied Science and Technology https://doi.org/10.38094/jastt1457 Trends, 1(4), 140–147.

8. Barrios, J. M., and Romero, P. E. (2019). Decision Tree Methods for Predicting Surface Roughness in Fused Deposition Modeling Parts. Materials, 12(16), 2574. https://doi.org/10.3390/ma12162574

9. F. Yılan, ̇I. B. S¸ ahin, F. Koc¸, and L. Urtekin, ”The Effects of Different Process Parameters of PLA+ on Tensile Strengths in 3D Printer Produced by Fused Deposition Modeling,” El-Cezerˆı Journal of Science and Engineering, vol. 10, no. 1, pp. 160-173, 2023. DOI: 10.31202/ecjse.1179492.

10. Thompson, B., et al. ”Hybrid Composite Materials in Additive Manufacturing.”Engineering Advances, 2021.

11. Garcia, F., et al. ”Cost-Effective Reinforcement Strategies for PLA.” Manufacturing Science Journal, 2020

12. Dawson, M., et al. ”Tensile and Impact Properties of PLA Composites.” Composite Structures, 2019

13. O'Connor, J., et al. "Investigating Metal Wire Reinforcement in Polymer Matrix."Materials Research, 2021.

14. Yu, S., et al. "Reinforcement of Thermoplastics Using Low-Cost Methods." Polymer Science Review, 2022.

15. Wu, Zhengyu et al. "State of the Art Review of Reinforcement Strategies and Technologies for 3D Printing of Concrete." Energies (2022): n. pag.

16. Sanei, S. H. R., and Popescu, D. (2020). 3D-Printed Carbon Fiber Reinforced Polymer Composites: A Systematic Review. Journal of Composites Science, doi:10.3390/jcs403009810.3390/jcs4030098

17. Hematibahar, Mohammad et al. "Influence of 3D-printed reinforcement on the-mechanical and fracture characteristics of ultra high performance concrete." Results in Engineering (2023): n. pag.

18. Boztoprak, Y. et al. (2024) 'Reinforcement of 3D printed PLA with carbon fiber reinforced composite and investigation of mechanical properties', Proceedings - The Twelfth International Symposium GRID 2024 [Preprint]. doi:10.24867/grid-2024-p45.

19. Maurya, S. et al. (2023) 'Inline reinforcement of steel cable in 3D Concrete Printing', Materials Today: Proceedings [Preprint]. doi:10.1016/j.matpr.2023.04.092.

20. Jahangir, M.N. et al. (2019) 'Reinforcement of material extrusion 3D printed polycarbonate using continuous carbon fiber', Additive Manufacturing, 28, pp.354–364. doi:10.1016/j.addma.2019.05.019.

21. T. Ambone, A. Torris, and K. Shanmuganathan, "Enhancing the mechanical properties of 3D printed polylactic acid using nanocellulose," Polymer Engineering & Science, vol. 60, no. 8, pp. 18421855,2020.4spepublications.onlinelibrary.wiley.com

22. M. El Moumen, M. Tarfaoui, and K. Lafdi, "Additive manufacturing of polymer composites: Processing and modeling approaches," Composites Part B: Engineering, vol. 171, pp. 166-182, 2019.

23. S. Hsueh, C. Lai, and C. Huang, "Comparative study on the mechanical properties of polylactic acid and polyethylene terephthalate glycol-modified 3D printed parts under various printing parameters," Journal of Materials Research and Technology, vol. 9, no. 6, pp. 14679-14688, 2020.

24. A. V. Dudescu and S. Racz, "Effects of raster orientation, infill rate and infill pattern on the mechanical properties of 3D printed materials," Acta Universitatis Cibiniensis, vol. 69, no. 1, pp. 2017.

25. T. A. Osswald and L. Menges, Material Science of Polymers for Engineers, 3rd ed., Munich: Hanser Publications, 2012.

26. M. Domingo-Espin, J. Puigoriol-Forcada, A. Garcia-Granada, J. Lluma`, and J. Borros, "Mechanical property characterization and simulation of fused deposition modeling Polycarbonate parts," Materials & Design, vol. 83, pp. 670-677, 2015.

27. A. M. Zahari, M. Z. M. Yusoff, and M. M. Ratnam, ”Mechanical properties and failure behavior of 3D printed carbon fiber reinforced polycarbonate under tensile and compressive loads,” Journal of Thermoplastic Composite Materials, vol. 34, no. 9, pp. 1237-1254, 2021.

28. D. Popescu, A. Zapciu, C. Amza, F. Baciu, and R. Marinescu, ”FDM process parameters influence over the mechanical properties of polymer specimens: A review,” Polymer Testing, vol. 69, pp. 157166, 2018.

29. G. X. Gu, M. Takaffoli, and M. J. Buehler, ”Hierarchically enhanced impact resistance of bioinspired composites,” Adv. Mater., vol. 29, no. 28, 2017.

30. J. J. Lewandowski and M. Seifi, ”Metal additive manufacturing: A review of mechanical properties,” Annu. Rev. Mater. Res., vol. 46, pp. 151–186, 2016.

31. T. M. Mower and M. J. Long, ”Mechanical behavior of additive manufactured, powder-bed laser-fused materials,” Mater. Sci. Eng. A, vol. 651, pp. 198–213, 2016.

32. L. A. Á vila Calderón et al., ”Creep and creep damage behavior of stainless steel 316L manufactured by laser powder bed fusion,” Mater. Sci. Eng. A, vol. 799, 2021.

33. A. Schmiedel et al., ”Very high cycle fatigue investigations on the fatigue strength of additive manufactured and conventionally wrought Inconel 718 at 873 K,” Metals, vol. 11, no. 11, 2021.

34. T. M. Smith, ”Efficient production of a high-performance dispersion strengthened, multi-principal element alloy,” Sci. Rep., vol. 10, 2020.

35. K.-T. Son et al., ”The creep and fracture properties of additively manufactured Inconel 625,” Materialia, vol. 15, 2021.

36. A. R. Studart, ”Biologically inspired dynamic material systems,” Angew. Chem. Int. Ed., vol. 54, no. 11, pp. 3400–3416, 2015.

37. M. D. Bartlett et al., ”High damping rubber composites with bioinspired hierarchical design,” Adv. Funct. Mater., vol. 26, no. 32, pp. 5961–5967, 2016.

38. S. Banerjee et al., ”Damping behavior of polymer matrix composites: A review,” J. Reinf. Plast. Compos., vol. 35, no. 9, pp. 716–736, 2016.

39. Y. Li et al., ”Vibration damping properties of polymer matrix composites based on carbon nanotube-modified epoxy,” Compos. Sci. Technol., vol. 151, pp. 153–160, 2017.

40. S. Lin et al., ”Dynamic and damping analysis of sandwich beams with magnetorheological elastomer cores under different loading conditions,” J. Sound Vib., vol. 442, pp. 190–204, 2019.